PHYTIC ACID ENRICHED BIOBASED MEMBRANES FOR LEAD ION REMOVAL FROM WATER

A Thesis
Submitted to the Graduate Faculty
of the
North Dakota State University
of Agriculture and Applied Science

By

Mayur Indal Ukey

In Partial Fulfillment of the Requirements
for the Degree of
MASTER OF SCIENCE

Major Department:
Coatings and Polymeric Materials

April 2021

Fargo, North Dakota

North Dakota State University
Graduate School

Title

PHYTIC ACID ENRICHED BIOBASED MEMBRANES FOR LEAD ION REMOVAL FROM WATER

By

Mayur Indal Ukey

The Supervisory Committee certifies that this ***disquisition*** complies with North Dakota State University's regulations and meets the accepted standards for the degree of

MASTER OF SCIENCE

SUPERVISORY COMMITTEE:

Dr. Mohiuddin Quadir
Chair

Dr. Dean C. Webster

Dr. Bakhtiyor Rasulev

Dr. Bezbaruah Achintya

Approved:

July 12, 2021
Date

Dr. Dean C. Webster
Department Chair

ABSTRACT

Pollution by heavy metals, such as lead (Pb), in bodies of water is a serious problem today that poses great risk to human health and the environment. In this study, cellulose-acetate (CA) based membranes were synthesized by immersion precipitation process, and commercially available CA membranes were modified by a layering method. Phytic acid (PA), a phosphorus rich compound known for its chelating properties, was doped into the membrane films to improve their efficiency in removing Pb (II) ions from water. As formulation additives, cellulose nanocrystals (CNCs), amine-functionalized cellulose nanofibers (CNFs) and chitosan were used. Mechanical properties, and filtration efficiency of the resulting membranes as a function of PA content, PA incorporation method, and additive types were assessed. Synthesized membrane films containing CNC, and chitosan/ PA coated membrane films showed up to 60% and 90% removal of Pb (II) ions respectively from water.

ACKNOWLEDGMENTS

I would like to thank my advisor Dr. Mohiuddin Quadir for all the helpful inputs provided in the research during my graduate studies. I also would like to thank my committee, Dr. Bakhtiyor Rasulev, Dr. Dean C. Webster, and Dr. Achintya Bezbaruah for being a very supportive committee. I would like to thank Corn Council for providing funds towards this project.

I would like to mention Tonoy Das and Wesley Kaeter for helping me with filtration experiments. Raj Hazra for helping me with synthesis. Dr. Scott Payne and Ms. Jayma Moore for capturing beautiful SEM images. Mr. Jim Bahr for XPS characterization. Dr. Chunju Gu and Mr. Greg Strommen for giving training on various characterization instrument.

Finally, I would like to express my thanks towards all the faculty, staff and students of the Coatings and Polymeric Department at North Dakota State University and the city of Fargo for providing a great educational experience.

TABLE OF CONTENTS

ABSTRACT iii

ACKNOWLEDGMENTS iv

LIST OF TABLES ix

LIST OF FIGURES x

CHAPTER 1: INTRODUCTION AND BACKGROUND 1

1.1. Introduction and Background 1

1.1.1. Types and sources of heavy metal in wastewater 1

1.1.2. Lead (Pb) as a heavy metal in wastewater 2

1.1.3. Impact of Pb (II) on human health 3

1.1.4. Burden statement of Pb (II) removal 3

1.1.5. Safe level of Pb (II) in water 4

1.2. Background of the Project 4

1.2.1. Current methods to remove heavy metals 4

1.2.2. Principles and mechanisms of membrane adsorptive systems 5

1.2.3. Introduction to biobased materials: advantages and shortcomings 6

1.2.3.1. Phytic acid (PA) 6

1.2.3.2. Cellulose 8

1.2.3.3. Cellulose acetate 9

1.2.3.4. Cellulose nanocrystals (CNC) 9

1.2.3.5. Cellulose nanofiber (CNF) 10

1.2.3.6. CNF-Amine 10

1.2.3.7. Chitosan 11

1.3. Overarching Goal of Our Project 11

1.4. Hypothesis of the Project 11

1.4.1. Specific aim of the project 12

1.4.2. Outline of the project 12

1.5. References 12

CHAPTER 2: PHYTIC ACID RICH CELLULOSE ACETATE BASED MEMBRANE PREPARED BY NON-SOLVENT INDUCED PHASE SEPARATION METHOD 23

2.1. Introduction 23

2.1.1. Background 23

2.1.2. Literature review 24

2.1.3. Principle 25

2.1.4. Goal of the project 25

2.2. Materials and Methods 26

2.2.1. Materials 26

2.2.2. Membrane fabrication using cellulose nanocrystals (CNC) 26

2.2.3. Synthesis of CNF-Amine 27

2.2.4. Membrane fabrication using CNF-Amine 27

2.2.5. Membrane fabrication using chitosan 28

2.3. Characterization 29

2.3.1. Mechanical properties 29

2.3.2. Pore size analysis 29

2.3.3. Elemental compositional evaluation 30

2.3.4. Filtration capacity evaluation 30

2.4. Results and Discussion 31

2.4.1. Mechanical properties 31

2.4.2. Pore size analysis 34

2.4.3. Compositional evaluation 34

2.4.4. Filtration capacity evaluation 36

2.5. Conclusion 36

2.6. Future Work 37

2.7. References 37

CHAPTER 3: LAYER BY LAYER IMMOBILIZATION OF PHYTIC ACID ON CELLULOSE ACETATE BASED MEMBRANES 40

3.1. Introduction 40

3.1.1. Background 40

3.1.2. Principle 42

3.1.3. Goal of our project 42

3.2. Materials and Methods 42

3.2.1. Materials 42

3.2.2. Preparation of dipped layer by layer using cellulose nanocrystal and phytic acid 43

3.2.3. Synthesis of CNF-Amine 43

3.2.4. Preparation of dipped layer by layer using CNF-Amine and phytic acid 43

3.2.5. Preparation of dipped layer by layer using chitosan and phytic acid 43

3.3. Characterization Methods 44

3.3.1. Mechanical properties 44

3.3.2. Porosity and microstructure 44

3.3.3. Surface phosphorus mapping 45

3.3.4. Surface elemental composition 45

3.3.5. Filtration capacity analysis 46

3.4. Results and Discussions 47

3.4.1. Mechanical properties 47

3.4.2. Porosity and microstructure 48

3.4.3. Surface phosphorus mapping 49

3.4.4. Surface elemental composition 50

3.4.5. Filtration capacity evaluation 50

3.5. Conclusion 51

3.6. Overall Conclusion 52

3.7. Challenges and Future Outlook 52

3.8. References..53

LIST OF TABLES

Table		Page
1.1:	Various systems for the adsorption of Pb (II)	5
1.2:	Dissociation constants of PA reported in literature	7
2.1:	Formulation containing CNC	26
2.2:	Formulation containing CNF-Amine	28
2.3:	Formulation containing chitosan	28

LIST OF FIGURES

Figure Page

1.1: Sources of heavy metal pollution 2

1.2: Lead (Pb) in periodic table 2

1.3: Effects of Pb (II) on human body 3

1.4: Phytic acid (PA) 7

1.5: Schematic representation of Pb-phosphate binding 8

1.6: Cellulose 9

1.7: Cellulose acetate 9

1.8: CNF-Amine 11

1.9: Chitosan 11

2.1: Non-solvent phase inversion casting process by [2] is licensed under CC BY 4.0 24

2.2: Reaction scheme of CNF-Amine 27

2.3: SEM image of (a) the membrane film, and (b) histogram of pore size diameter 30

2.4: Pb (II) ions containing water solution passing through filtration device 31

2.5: Cellulose acetate based membrane films 32

2.6: Mechanical properties of the film prepared using (a-c) CNC, (d-f) CNF-Amine, and (g-i) chitosan 33

2.7: Average pore size of the membrane films containing (a) CNC, (b) CNF-Amine, and (c) chitosan 34

2.8: Phosphorus content in the films containing (a) CNC, (b) CNF-Amine, and (c) chitosan 35

2.9: Phosphorus content before and after immersion precipitation in films blended with (a) CNC, (b) CNF-Amine, and (c) chitosan 35

2.10: % Pb (II) removal by the membrane films blended with (a) CNC, (b) CNF-Amine, and (c) chitosan 36

3.1: Layer-by-layer assembly techniques. Reprinted with permission from [2]. Copyright 2016 American Chemical Society. 41

3.2: SEM image of (a) the membrane film, and (b) histogram of pore size diameter 45

3.3: Pb (II) ions containing water solution passing through filtration device 47

3.4: Mechanical properties of the membrane films layered with (a - c) CNC/ PA, (d - f) CNF-Amine/ PA, and (g - i) chitosan/ PA 48

3.5: Average pore size of the membrane films layered with (a) CNC/ PA, (b) CNF-Amine/ PA, and (c) chitosan/ PA 49

3.6: Elemental maps of phosphorus on (a) control film, (b) DipLBL CHT-2, and (c) DipLBL CHT-5 49

3.7: Phosphorus content on the films layered with (a) CNC/ PA, (b) CNF-Amine/ PA, and (c) Chitosan/ PA 50

3.8: % Pb (II) removal by membrane films layered with (a) CNC/ PA, (b) CNF-Amine/ PA, and (c) chitosan/ PA 51

CHAPTER 1: INTRODUCTION AND BACKGROUND

1.1. Introduction and Background

Water makes up about two-thirds of the earth's surface, out of which less than one percent is fresh and accessible for use. The rest of the water is retained in oceans, glaciers, swamps, and other repositories that are not fit for direct use [1]. With an increasing world population, the demand for freshwater has also increased rapidly. Moreover, water mismanagement has led to reduced water quality on top of depleting water resources. Climate change has also presented us with water scarcity challenges [2].These interconnected water quality issues threaten the availability and accessibility of freshwater. This threat could potentially be offset by treating and reclaiming wastewater [3, 4].

1.1.1. Types and sources of heavy metal in wastewater

Wastewater is a result of natural and human activities in various occupations that leaves undesired things in water which cannot be further used for intended purpose [5]. The undesired things include large suspended particles, viruses, bacteria, colloids, monovalent and multivalent ions, dissolved organic matter, and dissolved salts whose sizes may vary from as small as in nanometers range to as big as visible to the naked eye [6]. One serious problem in the environment today is heavy metal contaminated water [7, 8]. Forces of nature such as wind and rain erode rocks and soil to release heavy metals in water bodies [9], and rapid industrial development such as mining, fertilizers, metal plating, batteries, pesticides, tanneries, etc., is responsible for heavy metal discharge into the environment [10]. These are non-biodegradable, toxic and carcinogenic. Commonly found heavy metals in wastewater are lead (Pb), arsenic (As), zinc (Zn), copper (Cu), mercury (Hg), cadmium (Cd), chromium (Cr), and nickel (Ni). These heavy metals have a negative impact on environment and human health. The presence of these heavy metals in human body above its critical level may result in health problems such as stomach cramps, vomiting, lung, kidney problems, and damage to the central nervous system, reproductive system, and brain function [11].

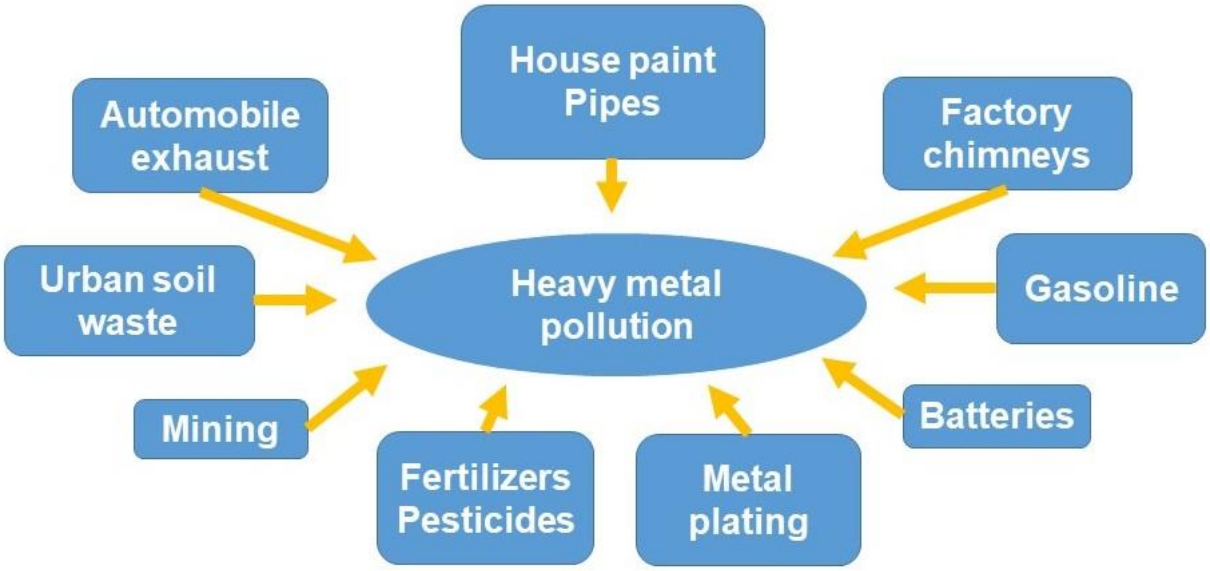

Figure 1.1: Sources of heavy metal pollution

1.1.2. Lead (Pb) as a heavy metal in wastewater

In the periodic table, Pb has an atomic number of 82 and an atomic weight of 207.2 dalton (Figure 1.2). Lead exists in two valence states of +2 and +4. Lead in oxidation state of +2 is more common. The main forms of lead found in the environment are elemental lead, organic lead, and lead salts. Various lead compounds exist in nature such as lead acetate, lead nitrate, lead arsenate, lead azide, lead sulfate to name a few [12]. Pb (II) in drinking water primarily comes from pipes, solder fittings, service connections to homes, faucets, and plumbing fixtures [13]. Lead compounds commonly found in drinking water are lead (II) oxide (PbO), lead (IV) oxide (PbO_2), lead (II) hydroxide ($Pb(OH)_2$), lead (II) carbonate ($PbCO_3$), lead (IV) carbonate ($Pb(CO_3)_2$) [14, 15].

Figure 1.2: Lead (Pb) in periodic table

1.1.3. Impact of Pb (II) on human health

Pb (II) has been widely used in industries because it is malleable, has low melting point, and is resistant to corrosion. Exposure to Pb (II) could result in cardiovascular diseases, hypertension, organ toxicities, miscarriages, and malformations. The damage caused by Pb (II) poisoning to human body is permanent and leads to death [16].

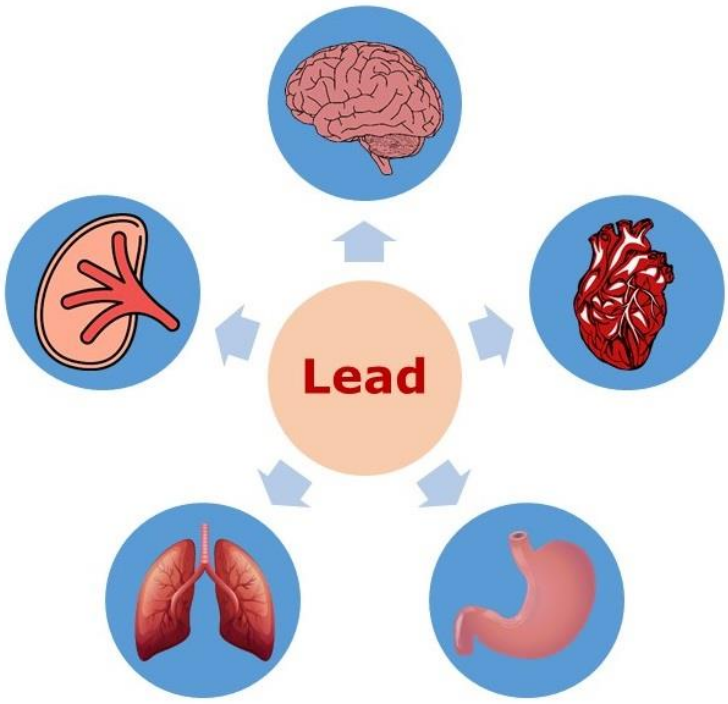

Figure 1.3: Effects of Pb (II) on human body

1.1.4. Burden statement of Pb (II) removal

In the 20th century, the main source of Pb (II) into the general population was from gasoline, paint, food, soil and dust. The exposure from these sources has been drastically reduced in recent years and no longer possess a serious threat. However, the exposure to Pb (II) from drinking water sources has increased. In the 21st century, two cases prove the same. First, the Pb (II) contamination in Washington D.C. drinking water during the year 2001-04, and second, in Flint, Michigan drinking water during the year 2014-16 [17]. Children were found to contain high levels of elevated blood lead (EBL) i.e. greater than 10 ppb in Washington DC areas leaving them with long lasting health risk. This was attributed to change

in the choice of disinfectant to chloramine from free chlorine. The new disinfectant caused the service line pipes to leach out Pb (II) [18]. The cost to replace the 23,000 lead pipes by District of Columbia Water and Sewer Authority (DCWASA), was estimated at $300 million [19]. The Flint water crisis showed a very high level of Pb (II) in water exceeding 5000 ppb. This level was caused by lack of corrosion control upon switching to Flint River from Detroit Water and Sewer Department [17, 20]. The repairing cost of the Flint water system was estimated at $1.5 billion [21].

1.1.5. Safe level of Pb (II) in water

In order to avoid health consequences due to contaminated drinking water, specialized agencies have regulated the amount of Pb (II) in drinking water with acceptable safety factor. The current drinking water standard set by the World Health Organization (WHO) is <10 µg/L and by the United States Environmental Protection Agency is <15 µg/L [13, 22].

1.2. Background of the Project

1.2.1. Current methods to remove heavy metals

Various methods have been extensively studied for the removal of heavy metals from wastewater. A few of the remediation technologies include chemical precipitation, ion-exchange, adsorption, coagulation-flocculation, electrochemical, floatation methods, and membrane filtration [23].

In the chemical precipitation technique, insoluble precipitates are formed upon the reaction of chemicals with heavy metal ions. An added step of sedimentation or filtration removes the precipitate giving clean water [24]. In the ion-exchange technique, ion-exchange resin is used to remove heavy metals by exchanging it with its cations [25]. Adsorption technique follows the physisorption or chemisorption mechanism for the removal of heavy metal ions. It offers the advantage of reuse after proper regeneration of adsorbent [26]. Coagulation-flocculation is another technique that involves destabilizing the colloids and forming flocs of large agglomerates [27]. In the electrochemical method, heavy metals are removed on an electrode surface with the use of electricity [28]. In the flotation technique,

gas bubbles are introduced in the solution. The suspended particles then get attached to the gas bubbles and move towards the surface of water where it is separated [29]. Membrane filtration is a technique where wastewater is passed through an inlet and with the mechanism of size exclusion, water without undesired particles is obtained at the outlet [23, 30].

Some of the examples of various techniques for the removal of Pb (II) found in literature are shown in Table 1.1.

Table 1.1: Various systems for the adsorption of Pb (II)

Material	Removal capacity	Method/ Mechanism	Ref
Hydrous manganese dioxide	204.1 mg/g	Electrostatic	[31]
Biological calcium carbonate	1667 mg/g	Chemisorption	[32]
Biochar anaerobic digested sludge	54.24 mg/g	Metal ion exchange and precipitation with minerals	[33]
Graphene oxide/ Chitosan aerogel	747.5 mg/g	Electrostatic interaction	[34]
Hydrogel membrane of graphene oxide and alginate	327.9 mg/g	Electrostatic attraction, chelation and ion-exchange	[35]
Hydrogel of carboxymethyl cellulose and polyacryamide	312.5 mg/g	Chemisorption	[36]
Pyromellitic dianhydride (PMDA) modified sugarcane bagasse, Na3PO4	241.7 mg/ g	Chemical precipitation	[37]
Nanoporous adsorbents of ZnO/ZnFe2O4/C	344.83 mg g−1	Ion-exchange	[38]

1.2.2. Principles and mechanisms of membrane adsorptive systems

A membrane is a selective barrier consisting of hollow pores that achieves separation by allowing particles smaller than its pore size to pass through it while excluding the particles larger than its pore size [39]. On the other hand, adsorption is a separation technique to exclude particles based on the affinity of the adsorbate with the adsorbent material [40]. Functionalizing a membrane with an adsorbent material could serve as an efficient dual-purpose separation technique [41].

1.2.3. Introduction to biobased materials: advantages and shortcomings

The most widely used polymers as membrane materials are polyethersulfone (PES), polyacrylonitrile (PAN), polypropylene (PP), polytetrafluoroethylene (PTFE), and polyvinylidine fluoride (PVDF) [42]. However, these materials are petroleum derived that could be detrimental to the environment. In recent years, there has been an increased attention towards renewable bio based materials from locally grown agricultural and forestry feedstock due to the increased depletion of non-renewable resources, increased awareness on sustainability, and abundance availability of biomass resources [43, 44]. Renewable resources are an interesting choice of materials because of its wide availability, renewability, degradability, reduced toxicity, and decreased footprint in the ecosystem [45, 46]. Inclusion of bio-based resources could help offset the disadvantages of the use petroleum based resources as, petroleum based products are responsible for rising amount of plastic waste, climate change, global warming, have increased carbon footprint, air and water pollution, are non-biodegradable, ends up in landfills, and plastics in the oceans are harmful for the fishes [47-49].

Taking into account the above discussion, a bio-based material selection approach was adopted to design and fabricate the membrane system. The membrane forming material was cellulose acetate. The heavy metal ion complexing material was phytic acid (PA). The additive materials were cellulose nanocrystals (CNC), cellulose nanofiber amine (CNF-Amine), and chitosan. In the following sections, properties of these materials are described.

1.2.3.1. Phytic acid (PA)

PA is a constituent of plants and is commonly found in cereals, legumes, nuts, grains, and seeds. It accounts up to 50-80% of total phosphorus in plants. This snowflake-like molecule has 6 phosphate groups with 12 replaceable protons. In the deprotonated form, it can form complex with positively charged multivalent cations [50].

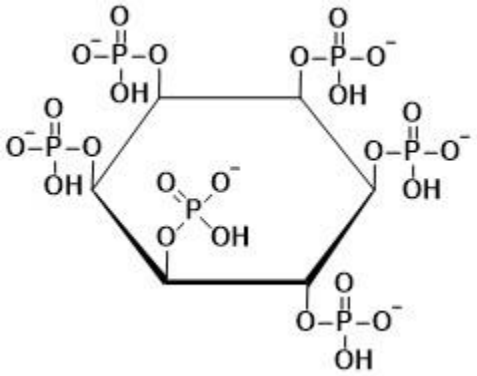

Figure 1.4: Phytic acid (PA)

The complexation of PA with metal ion depends on pH condition of the solution, molar ratio of metal to ligand, and the protonation level of the ligand [51]. Evans et al. observed that at an initial pH of 3.56, 5.3 mol Pb (II) could be accommodated per mol of PA and at an initial pH of 2.40, 4.7 mol of Pb (II) could be accommodated per mol of PA [52]. Brown et al. found that at a pH of above 5.6, 9 mol of Pb (II) could be accommodated per mol of PA and at lower pH of 2 and pH of 3, 4 mols of Pb (II) could be accommodated per mol of PA [53].

The strength of these complexes is determined by the dissociation constant of PA. Dissociation constants of PA measured using potentiometric titration reported by different authors are given in Table 1.2 [54].

Table 1.2: Dissociation constants of PA reported in literature

Authors	pK_a(1-6)	pK_a(7-8)	pK_a(9-12)	Ref
Andrews et al.	2.13	6.16	9.0	[55]
Barre et al	2.15	6.15	9.5	[56]
	1.84	5.84	9.73	
Costello et al	1.67	6.28	9.9	[57]
Lasztity et al	1.80	4.9	8.1	[54]

The complexation of PA has also been tested in several adsorptive system. For instance, when Cai et al. synthesized a $CoFe_2O_4$ magnetic adsorbent modified with PA, they found that the adsorption of Pb (II) onto the adsorbent was partly due to the chelating effect of PA with Pb (II) ions [58]. Another study by Lateef et al. showed adsorptive behavior and

corrosion inhibitive property of phytate on Pb and Pb-In alloy surfaces due to the chelating complex compound formation between PA active groups and Pb (II) ions [59]. The bonding of Pb (II) ions with the phytate group of PA is a result of combined effect of ion exchange, chelation and electrostatic attraction [58, 60, 61] and the schematic representation is presented in Figure 1.5.

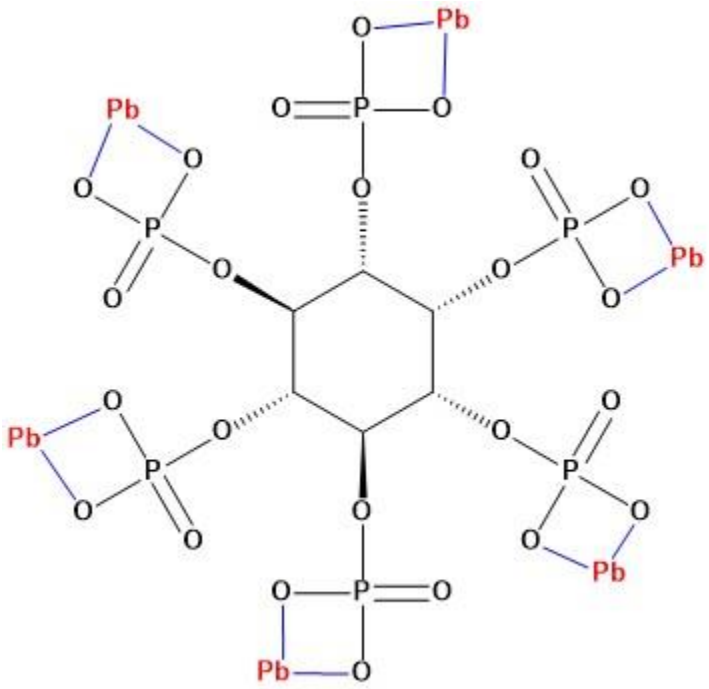

Figure 1.5: Schematic representation of Pb-phosphate binding

1.2.3.2. Cellulose

The most abundant, sustainable, and renewable polymer available in nature is cellulose. Composed of D-anhydroglucose units linked by β-(1-4)-glycosidic bonds, cellulose is a linear syndiotactic homopolymer. The presence of active sites in its structure, makes cellulose, a precursor for chemical and mechanical modifications. Cellulose is an inexpensive material available in abundance, has high aspect ratio and low density [62]. Environmental awareness is driving research towards the use and transformation of naturally occurring sustainable biomaterials such as cellulose. Some of the forms of cellulose are cellulose

nanofibers, cellulose nanocrystals, bacterial cellulose, electrospun cellulose nanofibers, and microfibrillated cellulose [63].

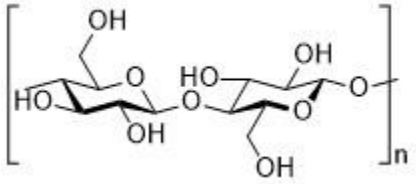

Figure 1.6: Cellulose

1.2.3.3. Cellulose acetate

Cellulose acetate is a common choice of material for preparing water filtration membrane because of its desirable physical properties. It is derived from cellulose, a renewable material. Cellulose acetate is widely available, biocompatible, non-toxic in nature, has good desalting properties, has high potential flux, toughness, modulus, flexural and mechanical strength, has favorable selectivity-permeability characteristics, thermal properties, easy processability and is low in cost [64-67].

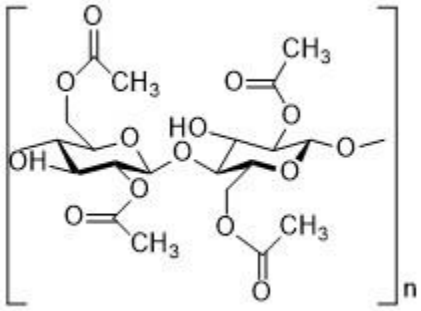

Figure 1.7: Cellulose acetate

1.2.3.4. Cellulose nanocrystals (CNC)

Acid hydrolysis of cellulose fibers using hydrochloric acid, phosphoric acid, or sulfuric acid produces CNC. This process distorts hydrogen bonds, breaks the amorphous regions, and releases crystalline rods. Depending upon the source of cellulose, and the hydrolysis conditions, cellulose of different morphologies are obtained with their rod-like structure showing a dimension of 10-20 nm and length of a few hundred [68]. Depending on the origin of cellulose and hydrolysis conditions, CNCs come in various dimensions. CNC properties are

determined by its degree of crystallinity and aspect ratio (length to diameter ratio). CNC is biodegradable, has good mechanical strength, high specific surface area, and has large amount of active sites for modification [68, 69].

1.2.3.5. Cellulose nanofiber (CNF)

Mechanical shearing techniques such as refining, grinding, and high-pressure homogenization are applied on cellulose pulp fibers to produced cellulose nanofibrils. Pretreatments facilitating disintegrating of the fibers have also been proposed such as oxidation, acidic and enzymatic treatment. The pretreatment principles consists of weakening hydrogen bonds, addition of repulsive charge, and lowering degree of polymerization. The methodology and type of pretreatment used determines the dimensions of CNF. CNFs produced are of diameters 20-40 nm that could be reduced down to 3-5 nm with appropriate pretreatment process and has a length of several micrometers [68].

Cellulose nanomaterials are promising materials for membranes because they offer high mechanical strength, surface area, chemical inertness, and hydrophilicity. Also, its hydrophilicity reduces bio-fouling, and organic fouling [70].

1.2.3.6. CNF-Amine

Since, the objective was to immobilize PA into the membrane system, CNF modified with amine was used. The amine group would form a complex with PA and the PA would further be used to chelate heavy metal ions from wastewater solution [71]. CNF-amine was synthesized according to the procedures reported by Dong et al. [72, 73].

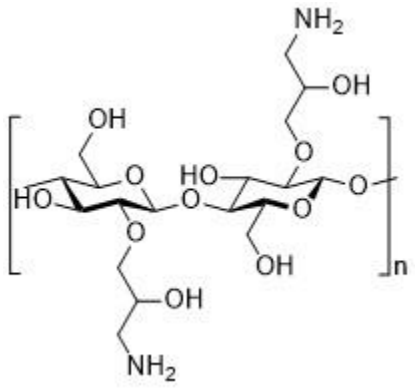

Figure 1.8: CNF-Amine

1.2.3.7. Chitosan

Chitosan is another biopolymer that is biodegradable, non-toxic, hydrophilic, cheap and readily available in nature. Certain disadvantages associated with chitosan is its low mechanical property, surface area, and thermal stability. Because it has several hydroxyl and amine groups attached to it, it has been used for the removal of heavy metals ions [74].

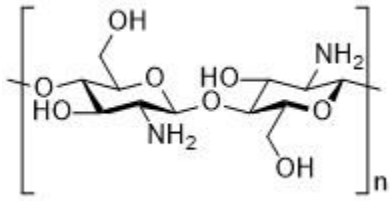

Figure 1.9: Chitosan

1.3. Overarching Goal of Our Project

The overarching goal of the project is to prepare a water filtration membrane from biobased resources for efficient capture Pb (II) from wastewater.

1.4. Hypothesis of the Project

The hypothesis of the project is that, by successful incorporation of PA into the cellulose acetate based membrane matrix, the chelating ability of PA could be utilized to improve the efficiency of the porous membrane in removing Pb (II) ions from the water.

1.4.1. Specific aim of the project

The specific aims are:

a) To prepare cellulose acetate-based films blended with PA and three reinforcing agents i.e. CNC, CNF-Amine, and chitosan.

b) To coat cellulose acetate-based films using layer-by-layer coating techniques using combinations such as CNC/ PA, CNF-Amine/ PA, and chitosan/ PA as layering materials with complementary electrical charge.

1.4.2. Outline of the project

In the following chapters, films made using non-solvent induced phase separation are described and then films modified using the layering technique are discussed.

1.5. References

[1] "How much water is there on Earth?" United States Geological Survey. (accessed 25th October, 2020).

[2] A. R. Sapkota, "Water reuse, food production and public health: Adopting transdisciplinary, systems-based approaches to achieve water and food security in a changing climate," *Environmental Research,* vol. 171, pp. 576-580, 2019/04/01/ 2019, doi: https://doi.org/10.1016/j.envres.2018.11.003.

[3] S. S. Ashok, T. Kumar, and K. Bhalla, "Integrated Greywater Management Systems: A Design Proposal for Efficient and Decentralised Greywater Sewage Treatment," *Procedia CIRP,* vol. 69, pp. 609-614, 2018/01/01/ 2018, doi: https://doi.org/10.1016/j.procir.2017.11.098.

[4] A. E. Burakov *et al.*, "Adsorption of heavy metals on conventional and nanostructured materials for wastewater treatment purposes: A review," *Ecotoxicology and Environmental Safety,* vol. 148, pp. 702-712, 2018/02/01/ 2018, doi: https://doi.org/10.1016/j.ecoenv.2017.11.034.

[5] O. Akpor, G. O. Ohiobor, and T. Olaolu, "Heavy Metal Pollutants in Wastewater Effluents: Sources, Effects and Remediation," *Archives of Biochemistry and Biophysics,* vol. 2, p. 37, 2014.

[6] S. Hube *et al.*, "Direct membrane filtration for wastewater treatment and resource recovery: A review," *Science of The Total Environment,* vol. 710, p. 136375, 2020/03/25/ 2020, doi: https://doi.org/10.1016/j.scitotenv.2019.136375.

[7] C. Z. Zhang, B. Chen, Y. Bai, and J. Xie, "A new functionalized reduced graphene oxide adsorbent for removing heavy metal ions in water via coordination and ion exchange," *Separation Science and Technology,* vol. 53, no. 18, pp. 2896-2905, 2018/12/12 2018, doi: 10.1080/01496395.2018.1497655.

[8] G. K. Sarma, S. Sen Gupta, and K. G. Bhattacharyya, "Nanomaterials as versatile adsorbents for heavy metal ions in water: a review," *Environmental Science and Pollution Research,* vol. 26, no. 7, pp. 6245-6278, 2019/03/01 2019, doi: 10.1007/s11356-018-04093-y.

[9] T. Wang, J. Pan, and X. Liu, "Characterization of heavy metal contamination in the soil and sediment of the Three Gorges Reservoir, China," (in eng), no. 1532-4117 (Electronic).

[10] E. Bazrafshan, L. Mohammadi, A. Ansari-Moghaddam, and A. H. Mahvi, "Heavy metals removal from aqueous environments by electrocoagulation process– a systematic review," *Journal of Environmental Health Science and Engineering,* vol. 13, no. 1, p. 74, 2015/10/26 2015, doi: 10.1186/s40201-015-0233-8.

[11] J. Monisha, T. Tenzin, A. Naresh, B. M. Blessy, and N. B. Krishnamurthy, "Toxicity, mechanism and health effects of some heavy metals," (in English), *Interdisciplinary Toxicology,* vol. 7, no. 2, pp. 60-72, 01 Jun. 2014 2014, doi: https://doi.org/10.2478/intox-2014-0009.

[12] (2004). *Lead and Lead Compounds*. [Online] Available: https://ntp.niehs.nih.gov/ntp/roc/content/profiles/lead.pdf

[13] *Lead in Drinking-water,* W. H. Organization, 2011.

[14] "Lead (Pb) and water." https://www.lenntech.com/periodic/water/lead/lead-and-water.htm (accessed 06/19/2020, 2020).

[15] W. Pan, C. Pan, Y. Bae, and D. Giammar, "Role of Manganese in Accelerating the Oxidation of Pb(II) Carbonate Solids to Pb(IV) Oxide at Drinking Water Conditions," *Environmental Science & Technology,* vol. 53, no. 12, pp. 6699-6707, 2019/06/18 2019, doi: 10.1021/acs.est.8b07356.

[16] M. A. Assi, M. N. Hezmee, A. W. Haron, M. Y. Sabri, and M. A. Rajion, "The detrimental effects of lead on human and animal health," (in eng), no. 0972-8988 (Print).

[17] S. Roy and M. A. Edwards, "Preventing another lead (Pb) in drinking water crisis: Lessons from the Washington D.C. and Flint MI contamination events," *Current Opinion in Environmental Science & Health,* vol. 7, pp. 34-44, 2019/02/01/ 2019, doi: https://doi.org/10.1016/j.coesh.2018.10.002.

[18] M. Edwards, S. Triantafyllidou, and D. Best, "Elevated Blood Lead in Young Children Due to Lead-Contaminated Drinking Water: Washington, DC, 2001−2004," *Environmental Science & Technology,* vol. 43, no. 5, pp. 1618-1623, 2009/03/01 2009, doi: 10.1021/es802789w.

[19] D. Nakamura. "WASA to Replace 2,800 Lead Pipes Over Next Year." Washington Post. (accessed May-01, 2021).

[20] K. J. Pieper, M. Tang, and M. A. Edwards, "Flint Water Crisis Caused By Interrupted Corrosion Control: Investigating “Ground Zero” Home," *Environmental Science & Technology,* vol. 51, no. 4, pp. 2007-2014, 2017/02/21 2017, doi: 10.1021/acs.est.6b04034.

[21] L. O. Gostin, "Politics and Public Health: The Flint Drinking Water Crisis," (in eng), no. 1552-146X (Electronic).

[22] "Ground Water and Drinking Water." United States Environmental Protection Agency. (accessed 25th October, 2020).

[23] F. Fu and Q. Wang, "Removal of heavy metal ions from wastewaters: A review," *Journal of Environmental Management,* vol. 92, no. 3, pp. 407-418, 2011/03/01/ 2011, doi: https://doi.org/10.1016/j.jenvman.2010.11.011.

[24] Z. Xu, S. Gu, D. Rana, T. Matsuura, and C. Q. Lan, "Chemical precipitation enabled UF and MF filtration for lead removal," *Journal of Water Process Engineering,* vol. 41, p. 101987, 2021/06/01/ 2021, doi: https://doi.org/10.1016/j.jwpe.2021.101987.

[25] K. Srinivasa Rao, P. K. Dash, D. Sarangi, G. Roy Chaudhury, and V. N. Misra, "Treatment of wastewater containing Pb and Fe using ion-exchange techniques," *Journal of Chemical Technology & Biotechnology,* https://doi.org/10.1002/jctb.1258 vol. 80, no. 8, pp. 892-898, 2005/08/01 2005, doi: https://doi.org/10.1002/jctb.1258.

[26] A. Das, N. Bar, and S. K. Das, "Pb(II) adsorption from aqueous solution by nutshells, green adsorbent: Adsorption studies, regeneration studies, scale-up design, its effect on biological indicator and MLR modeling," *Journal of Colloid and Interface Science,* vol. 580, pp. 245-255, 2020/11/15/ 2020, doi: https://doi.org/10.1016/j.jcis.2020.07.017.

[27] F. M. Pang, P. Kumar, T. T. Teng, A. K. Mohd Omar, and K. L. Wasewar, "Removal of lead, zinc and iron by coagulation–flocculation," *Journal of the Taiwan Institute of Chemical Engineers,* vol. 42, no. 5, pp. 809-815, 2011/09/01/ 2011, doi: https://doi.org/10.1016/j.jtice.2011.01.009.

[28] O. Surucu, "Trace determination of heavy metals and electrochemical removal of lead from drinking water," *Chemical Papers,* 2021/04/20 2021, doi: 10.1007/s11696-021-01662-3.

[29] W. Peng, G. Han, Y. Cao, K. Sun, and S. Song, "Efficiently removing Pb(II) from wastewater by graphene oxide using foam flotation," *Colloids and Surfaces A:*

Physicochemical and Engineering Aspects, vol. 556, pp. 266-272, 2018/11/05/ 2018, doi: https://doi.org/10.1016/j.colsurfa.2018.08.043.

[30] M. T. Hoang *et al.*, "Fabrication of thin film nanocomposite nanofiltration membrane incorporated with cellulose nanocrystals for removal of Cu(II) and Pb(II)," *Chemical Engineering Science,* vol. 228, p. 115998, 2020/12/31/ 2020, doi: https://doi.org/10.1016/j.ces.2020.115998.

[31] R. Jamshidi Gohari, W. J. Lau, T. Matsuura, E. Halakoo, and A. F. Ismail, "Adsorptive removal of Pb(II) from aqueous solution by novel PES/HMO ultrafiltration mixed matrix membrane," *Separation and Purification Technology,* vol. 120, pp. 59-68, 2013/12/13/ 2013, doi: https://doi.org/10.1016/j.seppur.2013.09.024.

[32] X. Zhou *et al.*, "Biogenic Calcium Carbonate with Hierarchical Organic–Inorganic Composite Structure Enhancing the Removal of Pb(II) from Wastewater," *ACS Applied Materials & Interfaces,* vol. 9, no. 41, pp. 35785-35793, 2017/10/18 2017, doi: 10.1021/acsami.7b09304.

[33] S. H. Ho, Y. D. Chen, Z. K. Yang, D. Nagarajan, J. S. Chang, and N. Q. Ren, "High-efficiency removal of lead from wastewater by biochar derived from anaerobic digestion sludge," *Bioresource Technology,* vol. 246, pp. 142-149, 2017/12/01/ 2017, doi: https://doi.org/10.1016/j.biortech.2017.08.025.

[34] R. Yu, Y. Shi, D. Yang, Y. Liu, J. Qu, and Z. Z. Yu, "Graphene Oxide/Chitosan Aerogel Microspheres with Honeycomb-Cobweb and Radially Oriented Microchannel Structures for Broad-Spectrum and Rapid Adsorption of Water Contaminants," *ACS Applied Materials & Interfaces,* vol. 9, no. 26, pp. 21809-21819, 2017/07/05 2017, doi: 10.1021/acsami.7b04655.

[35] C. Bai, L. Wang, and Z. Zhu, "Adsorption of Cr(III) and Pb(II) by graphene oxide/alginate hydrogel membrane: Characterization, adsorption kinetics, isotherm and thermodynamics studies," (in eng), *International journal of biological*

macromolecules, vol. 147, pp. 898-910, 2020/03// 2020, doi: 10.1016/j.ijbiomac.2019.09.249.

[36] C. B. Godiya, X. Cheng, D. Li, Z. Chen, and X. Lu, "Carboxymethyl cellulose/polyacrylamide composite hydrogel for cascaded treatment/reuse of heavy metal ions in wastewater," *Journal of Hazardous Materials,* vol. 364, pp. 28-38, 2019/02/15/ 2019, doi: https://doi.org/10.1016/j.jhazmat.2018.09.076.

[37] J. Q. Tang, J. B. Xi, J. X. Yu, R. A. Chi, and J. D. Chen, "Novel combined method of biosorption and chemical precipitation for recovery of Pb2+ from wastewater," *Environmental Science and Pollution Research,* vol. 25, no. 28, pp. 28705-28712, 2018/10/01 2018, doi: 10.1007/s11356-018-2901-6.

[38] D. Chen, W. Shen, S. Wu, C. Chen, X. Luo, and L. Guo, "Ion exchange induced removal of Pb(ii) by MOF-derived magnetic inorganic sorbents," *Nanoscale,* 10.1039/C6NR00695G vol. 8, no. 13, pp. 7172-7179, 2016, doi: 10.1039/C6NR00695G.

[39] H. Strathmann, "Membrane separation processes," *Journal of Membrane Science,* vol. 9, no. 1, pp. 121-189, 1981/01/01/ 1981, doi: https://doi.org/10.1016/S0376-7388(00)85121-2.

[40] S. S. Fiyadh *et al.*, "Review on heavy metal adsorption processes by carbon nanotubes," *Journal of Cleaner Production,* vol. 230, pp. 783-793, 2019/09/01/ 2019, doi: https://doi.org/10.1016/j.jclepro.2019.05.154.

[41] L. Hao, N. Wang, C. Wang, and G. Li, "Arsenic removal from water and river water by the combined adsorption - UF membrane process," (in eng), no. 1879-1298 (Electronic).

[42] M. M. Pendergast and E. M. V. Hoek, "A review of water treatment membrane nanotechnologies," *Energy & Environmental Science,* 10.1039/C0EE00541J vol. 4, no. 6, pp. 1946-1971, 2011, doi: 10.1039/C0EE00541J.

[43] H. Gogoi, T. Leiviskä, E. Heiderscheidt, H. Postila, and J. Tanskanen, "Removal of metals from industrial wastewater and urban runoff by mineral and bio-based sorbents," *Journal of Environmental Management,* vol. 209, pp. 316-327, 2018/03/01/ 2018, doi: https://doi.org/10.1016/j.jenvman.2017.12.019.

[44] A. K. Mohanty, M. Misra, and L. T. Drzal, "Sustainable Bio-Composites from Renewable Resources: Opportunities and Challenges in the Green Materials World," *Journal of Polymers and the Environment,* vol. 10, no. 1, pp. 19-26, 2002/04/01 2002, doi: 10.1023/A:1021013921916.

[45] H. Sehaqui *et al.*, "Enhancing adsorption of heavy metal ions onto biobased nanofibers from waste pulp residues for application in wastewater treatment," *Cellulose,* vol. 21, no. 4, pp. 2831-2844, 2014/08/01 2014, doi: 10.1007/s10570-014-0310-7.

[46] P. Jia, H. Xia, K. Tang, and Y. A. O. Zhou, "Plasticizers Derived from Biomass Resources: A Short Review. LID - 10.3390/polym10121303 [doi] LID - 1303," (in eng), no. 2073-4360 (Electronic).

[47] V. Siracusa and I. Blanco, "Bio-Polyethylene (Bio-PE), Bio-Polypropylene (Bio-PP) and Bio-Poly(ethylene terephthalate) (Bio-PET): Recent Developments in Bio-Based Polymers Analogous to Petroleum-Derived Ones for Packaging and Engineering Applications," *Polymers,* vol. 12, no. 8, 2020, doi: 10.3390/polym12081641.

[48] F. Perera, "Pollution from Fossil-Fuel Combustion is the Leading Environmental Threat to Global Pediatric Health and Equity: Solutions Exist. LID - 10.3390/ijerph15010016 [doi] LID - 16," (in eng), no. 1660-4601 (Electronic).

[49] T. Väisänen, O. Das, and L. Tomppo, "A review on new bio-based constituents for natural fiber-polymer composites," *Journal of Cleaner Production,* vol. 149, pp. 582-596, 2017/04/15/ 2017, doi: https://doi.org/10.1016/j.jclepro.2017.02.132.

[50] G. T. Tsao, Y. Zheng, J. Lu, and C. S. Gong, "Adsorption of heavy metal ions by immobilized phytic acid," *Applied Biochemistry and Biotechnology,* vol. 63, no. 1, p. 731, 1997/03/01 1997, doi: 10.1007/BF02920471.

[51] G. Marolt, E. Gričar, B. Pihlar, and M. Kolar, "Complex Formation of Phytic Acid With Selected Monovalent and Divalent Metals," (in English), *Frontiers in Chemistry,* Original Research vol. 8, no. 857, 2020-September-23 2020, doi: 10.3389/fchem.2020.582746.

[52] W. J. Evans and C. J. Martin, "Interactions of inositol hexaphosphate with Pb(II) and Be(II). A calorimetric study. XVIII," *Journal of Inorganic Biochemistry,* vol. 45, no. 2, pp. 105-113, 1992/02/01/ 1992, doi: https://doi.org/10.1016/0162-0134(92)80004-F.

[53] E. C. Brown, M. L. Heit, and D. E. Ryan, "PHYTIC ACID: AN ANALYTICAL INVESTIGATION," *Canadian Journal of Chemistry,* vol. 39, no. 6, pp. 1290-1297, 1961/06/01 1961, doi: 10.1139/v61-163.

[54] L. Lásztity and R. Lásztity, "INVESTIGATION OF THE FORMATION OF PHYTATE-METAL COMPLEXES," vol. 32, 4 ed: *Period. Polytech. Chem. Eng*, Jan. 1988, pp. 299-304.

[55] J. C. Andrews and E. Herrarte, "STUDIES ON PHYTIN," *Journal of the Elisha Mitchell Scientific Society,* vol. 67, no. 1, pp. 45-53, 1951.

[56] J. E. Barre R Fau - Courtois, G. Courtois Je Fau - Wormser, and G. Wormser, "[Study of the structure of phytic acid by means of its titration curves and by means of the conductivity of its solutions]," (in fre), no. 0037-9042 (Print), doi: D - CLML: 5527:11165:358 OTO - NLM.

[57] A. J. R. Costello, T. Glonek, and T. C. Myers, "31P Nuclear magnetic resonance□pH titrations of myo-inositol hexaphosphate," *Carbohydrate Research,* vol. 46, no. 2, pp. 159-171, 1976/02/01/ 1976, doi: https://doi.org/10.1016/S0008-6215(00)84287-1.

[58] K. Cai, W. Shen, B. Ren, J. He, S. Wu, and W. Wang, "A phytic acid modified CoFe2O4 magnetic adsorbent with controllable morphology, excellent selective adsorption for dyes and ultra-strong adsorption ability for metal ions," *Chemical Engineering Journal,* vol. 330, pp. 936-946, 2017/12/15/ 2017, doi: https://doi.org/10.1016/j.cej.2017.08.009.

[59] H. M. A. El-Lateef, A. R. El-Sayed, H. S. Mohran, and H. A. S. Shilkamy, "Corrosion inhibition and adsorption behavior of phytic acid on Pb and Pb–In alloy surfaces in acidic chloride solution," *International Journal of Industrial Chemistry,* vol. 10, no. 1, pp. 31-47, 2019/03/01 2019, doi: 10.1007/s40090-019-0169-4.

[60] Y. Fang, X. Liu, X. Wu, X. Tao, and W. Fei, "Electrospun polyurethane/phytic acid nanofibrous membrane for high efficient removal of heavy metal ions," (in eng), *Environmental technology,* pp. 1-8, 2019/08// 2019, doi: 10.1080/09593330.2019.1652695.

[61] X. Fang *et al.*, "Rapid Enrichment and Sensitive Detection of Multiple Metal Ions Enabled by Macroporous Graphene Foam," *Analytical Chemistry,* vol. 89, no. 21, pp. 11758-11764, 2017/11/07 2017, doi: 10.1021/acs.analchem.7b03336.

[62] Z. Dai *et al.*, "Fabrication and Evaluation of Bio-Based Nanocomposite TFC Hollow Fiber Membranes for Enhanced CO2 Capture," *ACS Applied Materials & Interfaces,* vol. 11, no. 11, pp. 10874-10882, 2019/03/20 2019, doi: 10.1021/acsami.8b19651.

[63] Y. Wang, X. Wang, Y. Xie, and K. Zhang, "Functional nanomaterials through esterification of cellulose: a review of chemistry and application," *Cellulose,* vol. 25, no. 7, pp. 3703-3731, 2018/07/01 2018, doi: 10.1007/s10570-018-1830-3.

[64] S. Yang, Q. Zou, T. Wang, and L. Zhang, "Effects of GO and MOF@GO on the permeation and antifouling properties of cellulose acetate ultrafiltration membrane," *Journal of Membrane Science,* vol. 569, pp. 48-59, 2019/01/01/ 2019, doi: https://doi.org/10.1016/j.memsci.2018.09.068.

[65] H. Etemadi, R. Yegani, and M. Seyfollahi, "The effect of amino functionalized and polyethylene glycol grafted nanodiamond on anti-biofouling properties of cellulose acetate membrane in membrane bioreactor systems," *Separation and Purification Technology,* vol. 177, pp. 350-362, 2017/04/28/ 2017, doi: https://doi.org/10.1016/j.seppur.2017.01.013.

[66] Y. Tian *et al.*, "Electrospun membrane of cellulose acetate for heavy metal ion adsorption in water treatment," *Carbohydrate Polymers,* vol. 83, no. 2, pp. 743-748, 2011/01/10/ 2011, doi: https://doi.org/10.1016/j.carbpol.2010.08.054.

[67] W. N. R. Jami'an, H. Hasbullah, F. Mohamed, N. Yusof, N. Ibrahim, and R. R. Ali, "Effect of evaporation time on cellulose acetate membrane for gas separation," *IOP Conference Series: Earth and Environmental Science,* vol. 36, p. 012008, 2016/06 2016, doi: 10.1088/1755-1315/36/1/012008.

[68] R. E. Abouzeid, R. Khiari, N. El-Wakil, and A. Dufresne, "Current State and New Trends in the Use of Cellulose Nanomaterials for Wastewater Treatment," *Biomacromolecules,* vol. 20, no. 2, pp. 573-597, 2019/02/11 2019, doi: 10.1021/acs.biomac.8b00839.

[69] N. Grishkewich, N. Mohammed, J. Tang, and K. C. Tam, "Recent advances in the application of cellulose nanocrystals," *Current Opinion in Colloid & Interface Science,* vol. 29, pp. 32-45, 2017/05/01/ 2017, doi: https://doi.org/10.1016/j.cocis.2017.01.005.

[70] P. R. Sharma, S. K. Sharma, T. Lindström, and B. S. Hsiao, "Nanocellulose-Enabled Membranes for Water Purification: Perspectives," *Advanced Sustainable Systems,* vol. 4, no. 5, p. 1900114, 2020/05/01 2020, doi: 10.1002/adsu.201900114.

[71] T. Zhang *et al.*, "Chitosan/Phytic Acid Polyelectrolyte Complex: A Green and Renewable Intumescent Flame Retardant System for Ethylene–Vinyl Acetate Copolymer," *Industrial & Engineering Chemistry Research,* vol. 53, no. 49, pp. 19199-19207, 2014/12/10 2014, doi: 10.1021/ie503421f.

[72] S. Dong and M. Roman, "Fluorescently Labeled Cellulose Nanocrystals for Bioimaging Applications," *Journal of the American Chemical Society,* vol. 129, no. 45, pp. 13810-13811, 2007/11/01 2007, doi: 10.1021/ja076196l.

[73] R. S. Hazra *et al.*, "Cellulose Mediated Transferrin Nanocages for Enumeration of Circulating Tumor Cells for Head and Neck Cancer," *Scientific Reports,* vol. 10, no. 1, p. 10010, 2020/06/19 2020, doi: 10.1038/s41598-020-66625-2.

[74] Sapna, R. Sharma, and D. Kumar, "Chapter 29 - Chitosan-Based Membranes for Wastewater Desalination and Heavy Metal Detoxification," in *Nanoscale Materials in Water Purification*, S. Thomas, D. Pasquini, S.-Y. Leu, and D. A. Gopakumar Eds.: Elsevier, 2019, pp. 799-814.

CHAPTER 2: PHYTIC ACID RICH CELLULOSE ACETATE BASED MEMBRANE PREPARED BY NON-SOLVENT INDUCED PHASE SEPARATION METHOD

2.1. Introduction

In this chapter, a facile fabrication method of immersion precipitation is utilized to prepare a cellulose acetate based asymmetric membrane. The membranes were reinforced with cellulose nanocrystals (CNC), cellulose nanofiber (CNF)-amine, and chitosan separately to act as a bridge between the membrane matrix and a chelating agent, Phytic Acid (PA). Several experiments with different formulations were conducted to reach successful modification of the membrane film with PA. Various characterization techniques such as tensile tester, SEM, ICP-OES, and atomic absorption spectroscopy were employed to check its physico-chemical properties, confirm the modification of the prepared membrane, and test its efficiency against a Pb (II) containing water solution.

2.1.1. Background

Non-solvent induced phase separation (NIPS) is the most common method for preparing flat sheet membranes. It consists of a casting solution containing a polymer, a good solvent, and additives, if any. The casting solution is first applied, using a casting knife, as a thin film on a mechanical support such as glass. The film and the support together are immersed in a coagulation bath containing poor solvent, i.e. a nonsolvent. The solvent and the nonsolvent are miscible with each other. The solvent and the nonsolvent exchange to solidify the polymer film [1]. A schematic diagram of the NIPS process is shown in Figure 2.1.

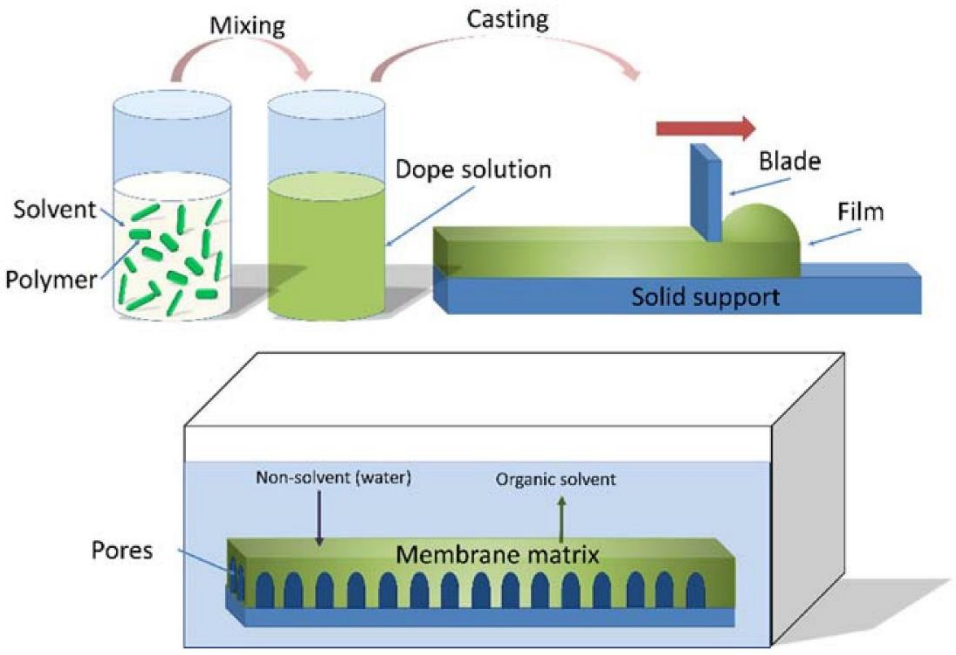

Figure 2.1: Non-solvent phase inversion casting process by [2] is licensed under CC BY 4.0

2.1.2. Literature review

Asymmetric membranes were first developed by Loeb and Sourirajan in the 1960s [3]. These membranes have been used in various separation application and industries such as food and dairy, textile, water treatment, beverage and semiconductors [1]. This method has been primarily employed for the preparation of flat sheet membrane and over the years several studies have been carried out to optimize the membrane design to suit its application.

Xu et al.et al., prepared ultrafiltration membranes of PVDF modified with a type of covalent organic framework made of 1,3,5-triformylbenzene and benzidine. The Pb (II) removal ability of the membrane was investigated with an initial Pb (II) concentration of 30 mg/L Pb $(NO_3)_2$/ water. The modified membrane was able to remove 92.4% of the initial concentration compared to 64% of unmodified membrane. Pore size decrement and top layer structural changes were attributed to the increase in the removal rate of Pb (II). The membrane also showed great antifouling property and high water flux [4].

Nayak et al., used the immersion precipitation technique to prepare flat sheet membranes of polyphenylsulfone and multiwalled carbon nanotubes. They used polyetherimide as a complexing agent to bind with Pb (II) and enhance the size of the metal ion. Their investigation showed that the Pb (II) removal efficiency by the membrane increased with increasing wt% of multiwalled carbon nanotubes. The separation was attributed to sieving mechanism [5].

Gohari et al, prepared a mixed matrix ultrafiltration membrane (MMM) of hydrous manganese dioxide (HMO) and polyethersulfone (PES) by varying the weight ratio. The increasing ratio of HMO to PES led to decrease in pore size but enhanced the flux that was caused by increase in hydrophilicity and porosity of the membrane. The highest Pb (II) uptake capacity of 204.1 mg of Pb(II)/g of MMM was demonstrated by the HMO:PES ratio of 2.0. The adsorption behavior was attributed to the electrostatic interactions of Pb(II) with Mn-OH group and inner sphere complex formation of Pb and O inside the MnO_6 octahedral structure [6].

2.1.3. Principle

In the immersion precipitation process, a liquid polymer solution is converted into a solid matter by liquid-liquid demixing in a coagulation bath through a gelation process. The solid membrane matrix results from the polymer rich phase while the pores in the membrane results from the polymer poor phase. The whole process is completed in a matter of few milliseconds [7].

2.1.4. Goal of the project

The goal of this project was to prepare a cellulose acetate-based membrane reinforced with bio-based materials such as cellulose nanocrystals, cellulose nanofiber-amine, and chitosan and immobilize phytic acid inside of it. Then test the efficiency of the prepared membranes by passing Pb (II) solution through it.

2.2. Materials and Methods

2.2.1. Materials

Cellulose acetate (CA, acetyl content 39.20 – 40.20 wt%, Mn 50,000), phytic acid solution 50% (w/w) in H_2O, 1-methyl-2-pyrrolidinone (NMP), polyvinylpyrrolidone (PVP), chitosan (CHT, 75-85% deacetylated, Mn 50,000 – 190,000 Da), sodium hydroxide (NaOH) and acetone was purchased from Sigma Aldrich. Cellulose nanocrystals (CNC) was supplied by the University of Maine. Cellulose nanofiber-amine (CNF-NH_3) was prepared in our lab according to the process described by Dong et al.[8].

2.2.2. Membrane fabrication using cellulose nanocrystals (CNC)

In a 20 ml glass reaction vial, 1.85 g of cellulose acetate, 0.15 g of CNC, 0.5 g of PVP, and 16 ml of NMP was added. To this reaction vial, phytic acid solution 50% (w/w) in H_2O in increasing concentrations of 0 ml, 0.4 ml, 0.8 ml, and 1.2 ml was further added. The formulation in wt% of reactant products is presented in Table 2.1. The solution was stirred overnight at room temperature so that the polymers would dissolve completely. After the complete dissolution of polymers, the solution was ultrasonicated for 3 hours to remove air bubbles. The casting solution was cast on a glass plate using a square drawdown bar with a gap clearance of 10 mils (254 µm). The film was immersed in a coagulation bath containing distilled water to produce a solidified film through the exchange of solvent and nonsolvent. The resulting membrane was heat-treated in water at 55°C for 2 hours to remove excess NMP. The membrane was allowed to air dry before testing.

Table 2.1: Formulation containing CNC

Formulation	Cellulose Acetate (g)	PVP (g)	CNC (g)	Phytic Acid (g)	NMP (ml)
CNC-P-0	1.85	0.15	0.5	0	16
CNC-P-1	1.85	0.15	0.5	0.272	16
CNC-P-2	1.85	0.15	0.5	0.544	16
CNC-P-3	1.85	0.15	0.5	0.816	16

(Phytic acid was used as 50% w/w solution in water)

2.2.3. Synthesis of CNF-Amine

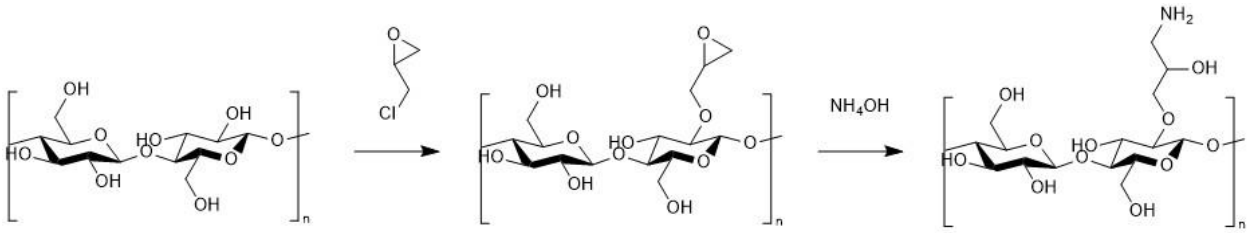

Figure 2.2: Reaction scheme of CNF-Amine

We adopted the method described by Dong et al. [8, 9]. Cellulose nanofibers were reacted with epichlorohydrin (6 mmol/g cellulose) in the presence of 1 M sodium hydroxide (132 mL/g cellulose) solution at 60°C for 2 hours under constant stirring. This reaction partially modified the hydroxyl group presence in cellulose backbone with epoxy functional group. Centrifugation followed by dialysis against deionized water was performed to through solvent and unreacted component out of the system. Modified cellulose nanofibers were maintained with pH~12 by 50% sodium hydroxide and further reacted with ammonium hydroxide at 60°C for 2 hours under constant stirring. Ammonium hydroxide reacted with epoxy functional groups and opened epoxy ring to introduce primary amine groups on the cellulose backbone. Final modified sample was dialyzed against deionized water to maintained pH~7 and stored for further application.

2.2.4. Membrane fabrication using CNF-Amine

In a 20 ml glass reaction vial, 1.50 g of cellulose acetate, 0.50 g of CNF-Amine, 0.5 g of PVP, and 16 ml of NMP was added. To this reaction vial, phytic acid solution 50% (w/w) in H_2O in increasing concentration of 0 ml, 0.4 ml, 0.8 ml, and 1.2 ml was further added. The formulation in wt% of reactant products is presented in Table 2.2. The solution was stirred overnight at room temperature so that the polymers would dissolve completely. After the complete dissolution of polymer, the solution was ultrasonicated for 3 hours to remove air bubbles. The casting solution was casted on a glass plate using a square drawdown bar with a gap clearance of 10 mils (254 μm). The film was immersed in a coagulation bath containing distilled water to produce a solidified film by the exchange of solvent and nonsolvent. The

obtained membrane was heat treated in water at 55°C for 2 hours to get rid of excess NMP. The membrane was allowed to air dry ready to be tested.

Table 2.2: Formulation containing CNF-Amine

Formulation	Cellulose Acetate (g)	PVP (g)	CNF-Amine (g)	Phytic Acid (g)	NMP (ml)
CNF-P-0	1.5	0.5	0.5	0	16
CNF-P-1	1.5	0.5	0.5	0.272	16
CNF-P-2	1.5	0.5	0.5	0.544	16
CNF-P-3	1.5	0.5	0.5	0.816	16

(Phytic acid was used as 50% w/w solution in water)

2.2.5. Membrane fabrication using chitosan

In a 20 ml glass reaction vial, 1.50 g of cellulose acetate, 0.50 g of chitosan, 0.5 g of PVP, and 16 ml of NMP was added. To this reaction vial, phytic acid solution 50% (w/w) in H_2O in increasing concentration of 0 ml, 0.4 ml, 0.8 ml, and 1.2 ml was further added. The formulation in wt% of reactant products are presented in Table 2.3. The solution was stirred overnight at room temperature so that the polymers would dissolve completely. After the complete dissolution of polymer, the solution was ultrasonicated for 3 hours to remove air bubbles. The casting solution was casted on a glass plate using a square drawdown bar with a gap clearance of 10 mils (254 μm). The film was immersed in a coagulation bath containing distilled water to produce a solidified film by the exchange of solvent and nonsolvent. The obtained membrane was heat treated in water at 55°C for 2 hours to get rid of excess NMP. The membrane was allowed to air dry ready to be tested.

Table 2.3: Formulation containing chitosan

Formulation	Cellulose Acetate (g)	PVP (g)	Chitosan (g)	Phytic Acid (g)	NMP (ml)
CHT-P-0	1.5	0.5	0.5	0	16
CHT-P-1	1.5	0.5	0.5	0.272	16
CHT-P-2	1.5	0.5	0.5	0.544	16
CHT-P-3	1.5	0.5	0.5	0.816	16

(Phytic acid was used as 50% w/w solution in water)

2.3. Characterization

2.3.1. Mechanical properties

The mechanical tests of the composite membranes were conducted according to ASTM D638, with Instron 5542 material testing instrument at temperature of 25°C. In this technique, a specimen is first cut into a specific shape and dimension, and fastened between two grips. It is then subjected to a pulling force until the specimen fractures, and its strength and elongation is determined. The membrane films were cut into Type V dimensions dog bone shape of width 3.18 mm, length 9.53 mm, and the draw speed was set at 0.5 mm/ min. The film was attached between two clamps of the machine. An average of three readings were recorded for tensile strength, tensile strain at break, and young's modulus to determine the mechanical property of the composite membranes.

2.3.2. Pore size analysis

Scanning electron microscope was used to capture microscopic images of the membrane films and analyze them on a microscopic scale. In this technique, high energy electron beam is passed through set of lenses on to the sample. The secondary and backscattered electrons generated from the sample is detected by the detector and a microscopic image is produced. Sample material was attached to cylindrical aluminum mounts with carbon adhesive tabs (Ted Pella, Redding, California, USA). Mounted specimens were sputter coated with a conductive layer of gold (Cressington 108auto, Ted Pella, Redding, California, USA). Images were obtained with a JEOL JSM-6490LV scanning electron microscope (JEOL USA, Inc., Peabody MA, USA).

The pore size of the films was calculated using the software Image J. An SEM image of a particular film was taken as shown in Figure 2.3 a. Circular shapes were drawn over the pores manually to calculate its area. Once all the pores of a particular image were taken into consideration, pore diameters were calculated from its obtained area and a histogram of pores diameter were plotted to calculate its mean diameter (Figure 2.3 b).

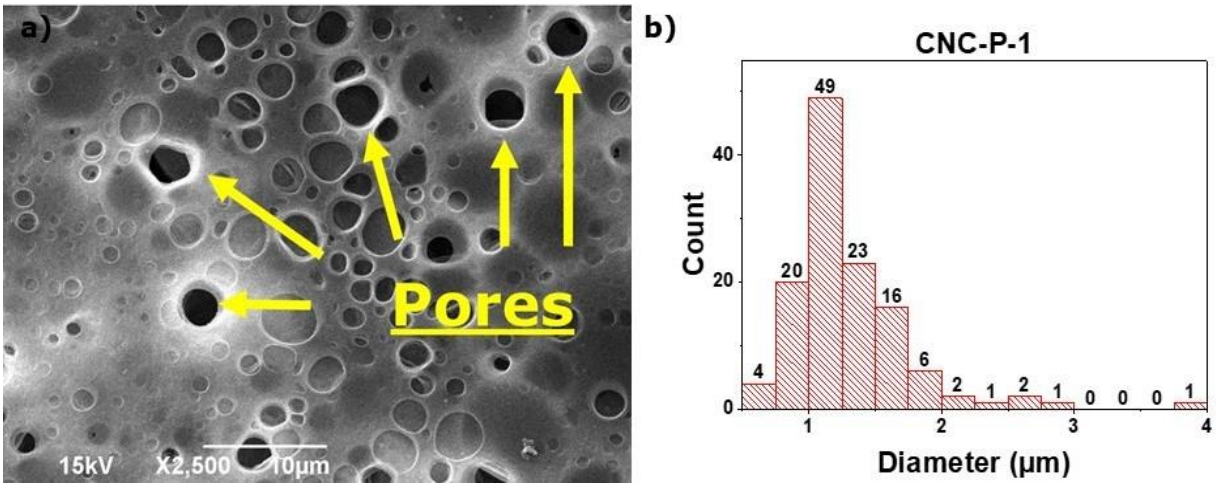

Figure 2.3: SEM image of (a) the membrane film, and (b) histogram of pore size diameter

2.3.3. Elemental compositional evaluation

Total phosphorus composition inside the membrane was found from inductively coupled plasma optical emission spectroscopy (Perkin Elmer Optima 8300 ICP-OES). This instrument is used to quantify the amount of a certain element in a sample. In this technique, the sample is run through a hot argon plasma. The sample emits light on excitation of atoms in the sample. Every element has a characteristic wavelength and the intensity provide details about the concentration of the element present in the sample.

The membrane samples were first weighed into fluoropolymer digestion tubes. 10 ml HNO_3 and 2 ml HCl were then added to the tube. The digestion tubes were then capped and placed in the microwave digestion system. Samples were then heated at 175°C for 5 minutes. After digestion, the digested product was brought to a volume of 50 ml using class A volumetric flask. Following EPA 6010 method guidelines, the phosphorus analysis was carried out in an ICP-OES.

2.3.4. Filtration capacity evaluation

Membrane films were cut into circular shape and fitted inside a polypropylene filter assembly of 25 mm diameter. A Pb (II) containing solution was prepared of concentration 1 mg Pb/ L of water. 100 ml Pb (II) solution was passed through the filter assembly at the rate

of 1 ml/ min and collected at the end for the evaluation of percentage removal of Pb (II) with Perkin Elmer atomic absorption spectroscopy – PinAAcle 900H.

Atomic absorption spectroscopy technique is used to measure trace elements present in a sample. In this technique, the element of interest absorbs light of specific wavelength from the cathode lamp, having a cathode made up of same element as the one being studied. The excited trace metal in the sample, while returning to its ground state, emits light with their characteristic wavelength and intensity, which helps to detect the metal and quantify its concentration.

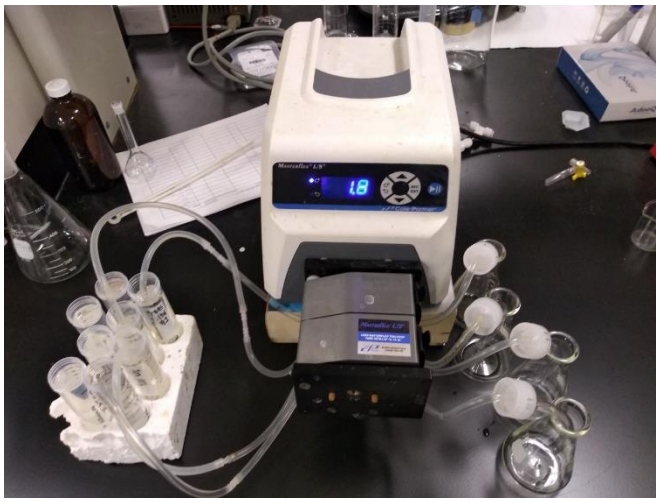

Figure 2.4: Pb (II) ions containing water solution passing through filtration device

2.4. Results and Discussion

2.4.1. Mechanical properties

To begin with, we first tested the mechanical properties of the dried membrane films. Figure 2.5. presents the dried membrane films after the immersion precipitation process. The membrane films receive stability and became flexible on addition of phytic acid, indicating that phytic acid also acts as a stabilizing agent. Such phenomenon is observed because the negatively charged phosphoric acid groups associate with the protonated carbonyl group of polyvinyl pyrrolidone by electrostatic interactions [10].

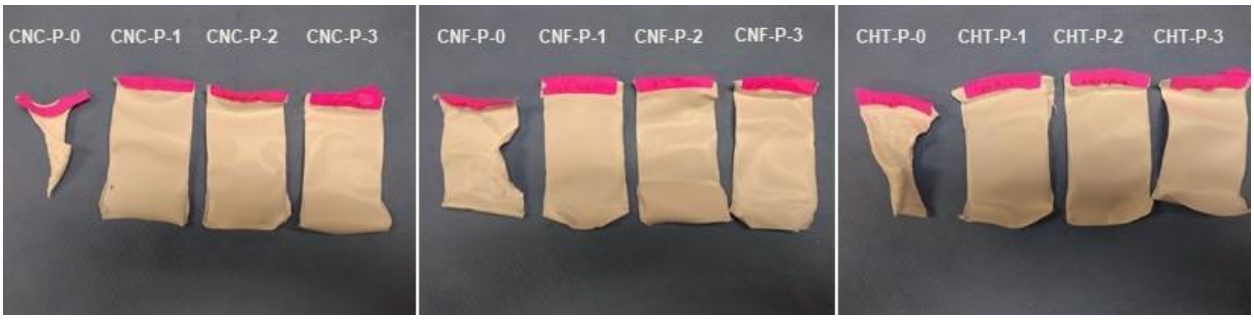

Figure 2.5: Cellulose acetate based membrane films

Figures 2.6 presents the mechanical properties of the composite membranes made using CNC, CNF-Amine, and Chitosan. The membranes were tested for their tensile stress, elongation at break, and young's modulus. The composition of the casting solution plays a vital role in the mechanical properties of the thin film membrane. The films CNC-P-0 and CHT-P-0, that contains no amount of phytic acid, wrinkled and did not form a flat sheet membrane, and therefore its mechanical properties could not be calculated.

As can be seen in figure 2.6 (a - c), the mechanical properties of the CNC blended membrane film improve with the rise in the concentration of phytic acid with highest value of tensile stress and Young's modulus obtained as 2.72 MPa and 40.26 MPa respectively. Phytic acid can form hydrogen bond with cellulose chains. Therefore, the increasing concentration of phytic acid promotes dimensional stability and explains the increasing trend in the mechanical properties of the CNC blended membrane film [11].

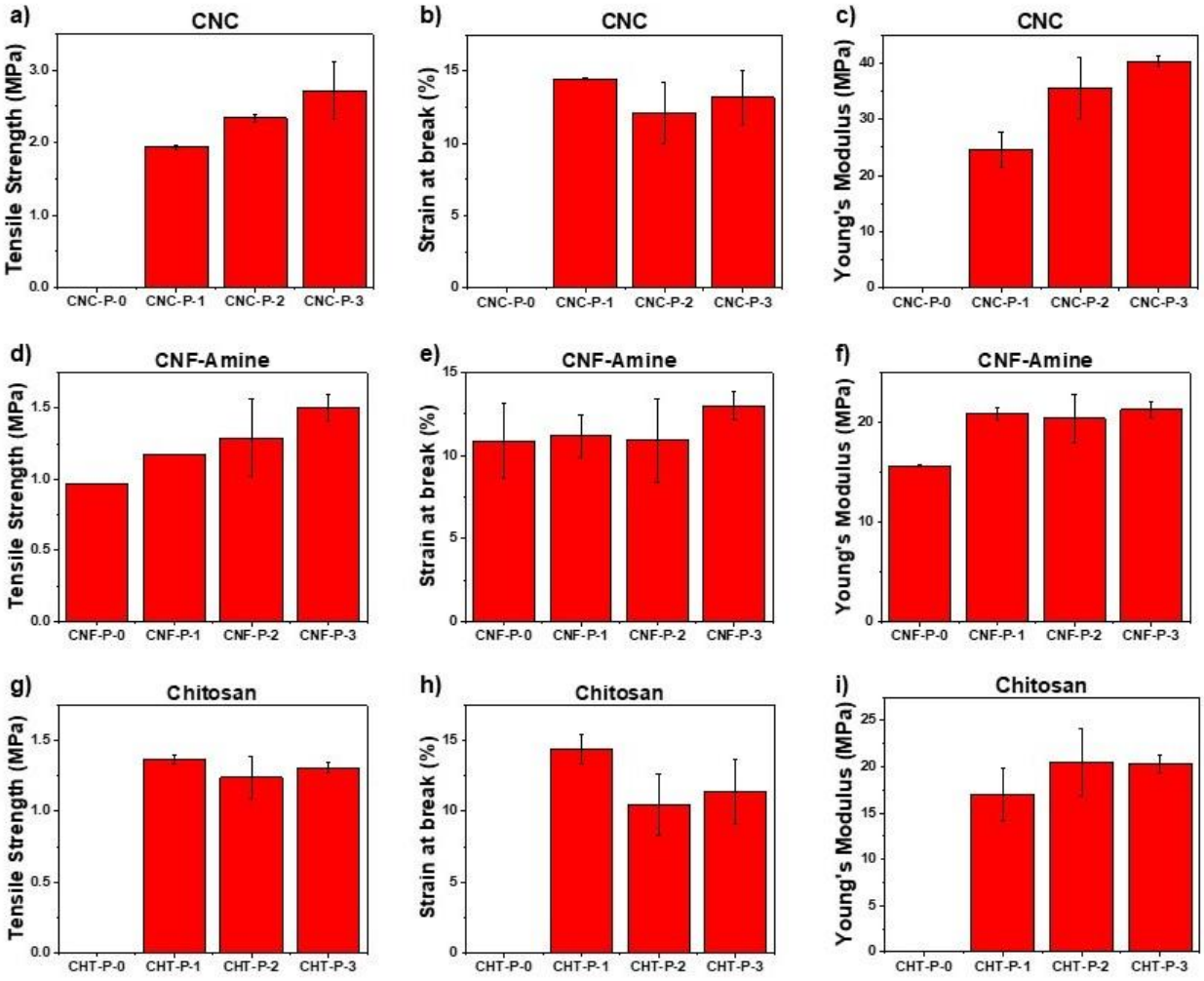

Figure 2.6: Mechanical properties of the film prepared using (a-c) CNC, (d-f) CNF-Amine, and (g-i) chitosan

CNF reinforces CA based polymer membrane because of high aspect ratio and good mechanical features. Also, CNF has relatively low density, is biodegradable, renewable, non-toxic, and cost-effective. The interfacial interaction between CNFs and CA matrix, explains good tensile strength and elongation at break. The hydrogen bonding between CNF and CA leads to rigid polymer structure enhancing mechanical properties [12]. Phytic acid forms hydrogen bonds with cellulose nanofibers and also with amine groups [11]. Therefore, in Figure 2.6 (d-f), an increase in the mechanical properties of the CNF-Amine blended membrane film is observed upon increasing the concentration of phytic acid.

In the case of chitosan blended films as shown in Figure 2.6 (g-i), there is no increasing or decreasing trend in the mechanical properties. The reason for such phenomenon could be uneven dispersion of chitosan in the solution that causes agglomeration of chitosan in the films and have an impact on the mechanical property of the membrane film.

On comparing the mechanical properties of the three different blended films, CNC blended films showed superior mechanical properties compared with CNF-Amine and chitosan blended films. Inclusion of phytic acid directly impacts CNC and CNF-Amine blended films in terms of its mechanical strength.

2.4.2. Pore size analysis

The average pore size for each of the films containing CNC, CNF-Amine, and chitosan are presented in Figure 2.7 a, 2.7 b, and 2.7 c respectively. The pore size for films containing CNC with no amount of phytic acid is not presented because no pores were formed on the top surface of the membrane. An enhancement in the pore size of the membrane containing CNC with the increase in the amount of phytic acid was observed [10]. However, in the case of CNF-Amine and chitosan containing membrane the results appear to be inconsistent with respect to phytic acid.

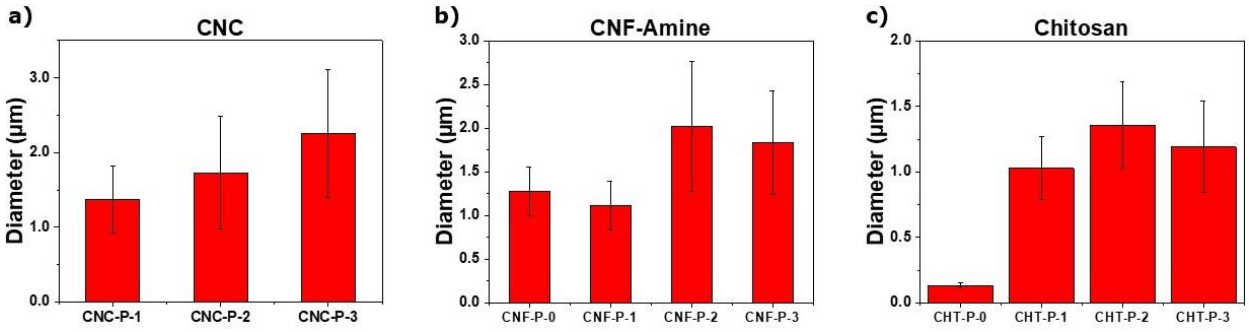

Figure 2.7: Average pore size of the membrane films containing (a) CNC, (b) CNF-Amine, and (c) chitosan

2.4.3. Compositional evaluation

Phosphorus content in the films were determined using inductively coupled plasma optical emission spectroscopy to establish the presence of phytic acid. Figure 2.8 a, 2.8 b,

and 2.8 c shows that phosphorus is present in the membrane film containing CNC, CNF-Amine, and chitosan respectively. Also, the amount of phosphorus content in the film increases with the increased addition of phytic acid. The presence of phosphorus in the membrane films is due to the formation of hydrogen bond by phytic acid with cellulose chains and amine group.

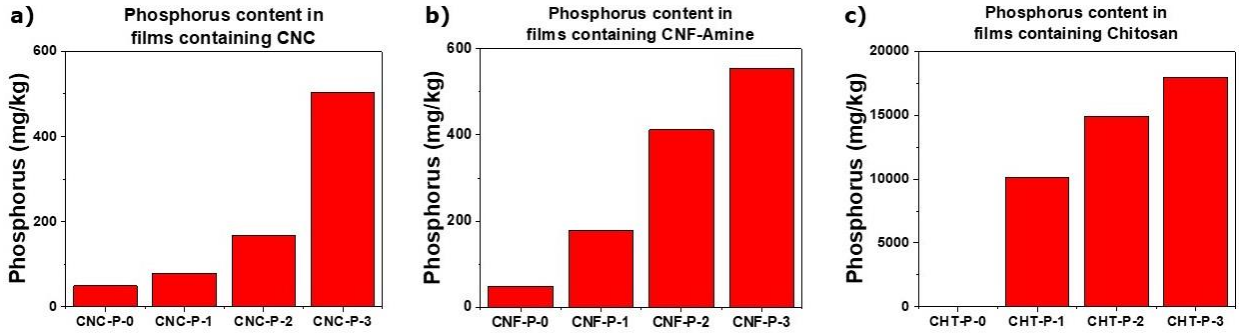

Figure 2.8: Phosphorus content in the films containing (a) CNC, (b) CNF-Amine, and (c) chitosan

Next, we compared the above ICP-OES results with the initial amount of phosphorus added to the casting solution. The initial amount of phosphorus added in the membrane film in an increasing quantity was 76,568 mg/kg (P-1), 153,417 mg/kg (P-2), and 229,704 mg/kg (P-3). The retention quantity is found to be the highest for the films containing chitosan (Figure 2.9 c), followed by CNF-Amine (Figure 2.9 b), and lastly CNC (Figure 2.9 a). The lost phytic acid from the membrane system could be due to its dispersion from thin film solution to water solution during the immersion precipitation process.

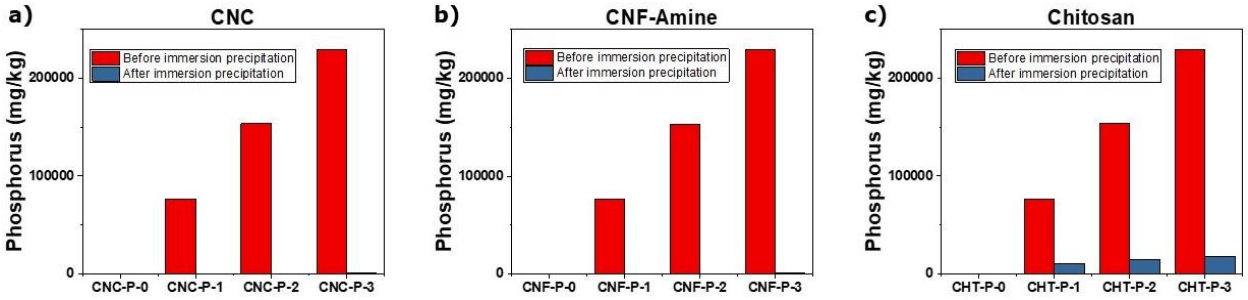

Figure 2.9: Phosphorus content before and after immersion precipitation in films blended with (a) CNC, (b) CNF-Amine, and (c) chitosan

2.4.4. Filtration capacity evaluation

In the filtration experiment, the films containing CNC are found to be performing better than the films containing CNF-Amine and chitosan (Figure 2.10). Films containing CNC showed up to 60% Pb (II) removal, which is approximately 3-fold better than the films containing CNF-Amine and chitosan. A possible reason for Pb (II) binding well in the films containing CNC could be the reactive hydroxyl groups of CNC where Pb (II) interacts electrostatically [13-15]. Even though the films containing CNF-Amine and chitosan contain more amount of phosphorus compared with films containing CNC, these films do not remove enough Pb (II) ions from the solution. This could be possibly because all the phosphate groups of phytic acid gets utilized with the primary amine of CNF-amine and chitosan leaving no interactive groups to bind with Pb (II) ions. While in the case of films blended with CNC, there could be remaining phosphate groups to bind with Pb (II) ions.

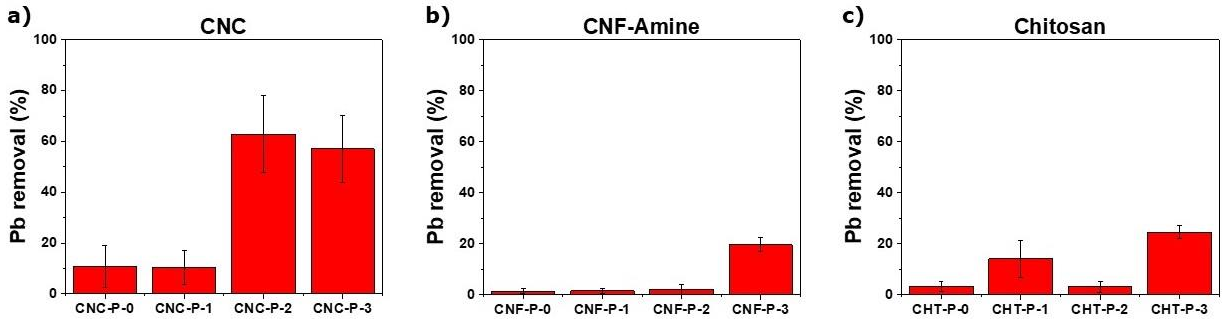

Figure 2.10: % Pb (II) removal by the membrane films blended with (a) CNC, (b) CNF-Amine, and (c) chitosan

2.5. Conclusion

Cellulose acetate-based films reinforced with CNC, CNF-Amine, and chitosan were successfully prepared. Phytic acid was successfully immobilized inside the membrane film. Films blended with CNC performed better in removing Pb (II) ions from water than the films blended with CNF-Amine and chitosan. This behavior could be attributed to the reactive hydroxyl groups of CNC on which Pb (II) ions binds electrostatically. There is a possibility that all the phosphate groups of phytic acid gets used up in binding with the primary amine groups of CNF-amine and chitosan leaving little to no opportunity to bind with Pb (II) ions. While in

the case of films blended with CNC, there could be available phosphate groups in the system for Pb (II) ions to bind with and enhance the membrane system to remove Pb (II) ions from water.

2.6. Future Work

The results can further be strengthened up by performing an X-ray photoelectron spectroscopy of the membrane films after the filtration experiment to check the residual amount of Pb (II) ions remaining in the filter membrane.

2.7. References

[1] G. R. Guillen, Y. Pan, M. Li, and E. M. V. Hoek, "Preparation and Characterization of Membranes Formed by Nonsolvent Induced Phase Separation: A Review," *Industrial & Engineering Chemistry Research,* vol. 50, no. 7, pp. 3798-3817, 2011/04/06 2011, doi: 10.1021/ie101928r.

[2] X. Dong, A. Al-Jumaily, and I. C. Escobar, "Investigation of the Use of a Bio-Derived Solvent for Non-Solvent-Induced Phase Separation (NIPS) Fabrication of Polysulfone Membranes," *Membranes,* vol. 8, no. 2, p. 23, 2018.

[3] S. Loeb and S. Sourirajan, "Sea Water Demineralization by Means of an Osmotic Membrane," in *Saline Water Conversion—II*, vol. 38, (Advances in Chemistry, no. 38): AMERICAN CHEMICAL SOCIETY, 1963, ch. 9, pp. 117-132.

[4] W. Xu, X. Sun, M. Huang, X. Pan, X. Huang, and H. Zhuang, "Novel covalent organic framework/PVDF ultrafiltration membranes with antifouling and lead removal performance," *Journal of Environmental Management,* vol. 269, p. 110758, 2020/09/01/ 2020, doi: https://doi.org/10.1016/j.jenvman.2020.110758.

[5] M. Chandrashekhar Nayak, A. M. Isloor, Inamuddin, B. Lakshmi, H. M. Marwani, and I. Khan, "Polyphenylsulfone/multiwalled carbon nanotubes mixed ultrafiltration membranes: Fabrication, characterization and removal of heavy metals Pb2+, Hg2+, and Cd2+ from aqueous solutions," *Arabian Journal of Chemistry,* vol. 13, no. 3, pp. 4661-4672, 2020/03/01/ 2020, doi: https://doi.org/10.1016/j.arabjc.2019.10.007.

[6] R. Jamshidi Gohari, W. J. Lau, T. Matsuura, E. Halakoo, and A. F. Ismail, "Adsorptive removal of Pb(II) from aqueous solution by novel PES/HMO ultrafiltration mixed matrix membrane," *Separation and Purification Technology,* vol. 120, pp. 59-68, 2013/12/13/ 2013, doi: https://doi.org/10.1016/j.seppur.2013.09.024.

[7] A. K. HoBda and I. Vankelecom, "Understanding and guiding the phase inversion process for synthesis of solvent resistant nanofiltration membranes," *Journal of Applied Polymer Science,* vol. 132, 2015.

[8] S. Dong and M. Roman, "Fluorescently Labeled Cellulose Nanocrystals for Bioimaging Applications," *Journal of the American Chemical Society,* vol. 129, no. 45, pp. 13810-13811, 2007/11/01 2007, doi: 10.1021/ja076196l.

[9] R. S. Hazra *et al.*, "Cellulose Mediated Transferrin Nanocages for Enumeration of Circulating Tumor Cells for Head and Neck Cancer," *Scientific Reports,* vol. 10, no. 1, p. 10010, 2020/06/19 2020, doi: 10.1038/s41598-020-66625-2.

[10] J. Hu *et al.*, "Phytic acid assisted preparation of high-performance supercapacitor electrodes from noncarbonizable polyvinylpyrrolidone," *Journal of Power Sources,* vol. 448, p. 227402, 2020/02/01/ 2020, doi: https://doi.org/10.1016/j.jpowsour.2019.227402.

[11] D. Xu, X. Xiao, J. Cai, J. Zhou, and L. Zhang, "Highly rate and cycling stable electrode materials constructed from polyaniline/cellulose nanoporous microspheres," *Journal of Materials Chemistry A,* 10.1039/C5TA03917G vol. 3, no. 32, pp. 16424-16429, 2015, doi: 10.1039/C5TA03917G.

[12] Y. Pan, L. Liu, L. Song, Y. Hu, S. Jiang, and H. Zhao, "Reinforcement of layer-by-layer self-assembly coating modified cellulose nanofibers to reduce the flammability of polyvinyl alcohol," *Cellulose,* vol. 26, no. 5, pp. 3183-3192, 2019/03/01 2019, doi: 10.1007/s10570-019-02298-z.

[13] N. Mohammed, N. Grishkewich, and K. C. Tam, "Cellulose nanomaterials: promising sustainable nanomaterials for application in water/wastewater treatment processes,"

Environmental Science: Nano, 10.1039/C7EN01029J vol. 5, no. 3, pp. 623-658, 2018, doi: 10.1039/C7EN01029J.

[14] J. Zhang, L. Li, Y. Li, and C. Yang, "Microwave-assisted synthesis of hierarchical mesoporous nano-TiO2/cellulose composites for rapid adsorption of Pb2+," *Chemical Engineering Journal,* vol. 313, pp. 1132-1141, 2017/04/01/ 2017, doi: https://doi.org/10.1016/j.cej.2016.11.007.

[15] S. Chen, W. Shen, F. Yu, W. Hu, and H. Wang, "Preparation of amidoximated bacterial cellulose and its adsorption mechanism for Cu2+ and Pb2+," *Journal of Applied Polymer Science,* https://doi.org/10.1002/app.31477 vol. 117, no. 1, pp. 8-15, 2010/07/05 2010, doi: https://doi.org/10.1002/app.31477.

CHAPTER 3: LAYER BY LAYER IMMOBILIZATION OF PHYTIC ACID ON CELLULOSE ACETATE BASED MEMBRANES

3.1. Introduction

The performance of membranes are restricted by their trade-off between permeability and selectivity. In order to improve upon the physicochemical characteristics, provide functionality, better selectivity as well as permeability, membrane materials are often modified to achieve targeted separation [1]. In this chapter, three different composite systems were used to layer a commercially available cellulose acetate-based membrane film by a dipping method. The first film system was coated with cellulose nanocrystals (CNC) and phytic acid (PA). The second one was coated with cellulose nanofiber (CNF)-amine and PA. And the third one was coated with chitosan and PA.

3.1.1. Background

A sequential layer-by-layer (LBL) assembly of materials of interest has been explored in various fields. There are a variety of LBL assembly technologies such as spin coating, spray coating, dipped coating, electromagnetic, vacuum or pressure assisted assembly and additive manufacturing [2]. Schematic representation of a few LBL technique is shown in Figure 3.1. Several studies have been carried out exploring the mentioned LBL assembly techniques.

For instance, S. Gao et al., used a LBL technique to create an ultrathin hydrogel on polyacrylic acid-grafted-poly (vinylidene fluoride) filtration membrane by applying multilayer coat of copper and alginate. They prepared this system to separate crude oil from water which required a strong hydration layer over membrane. So, they used alginate that had strong hydration ability. Using the LBL construction technique, they were able to control the thickness of the membrane at nanometer scale. The prepared membrane was able to separate crude oil from water at a water flux rate of 1230 L m^{-2} h^{-1} bar^{-1} at an efficiency of 99.8% [3].

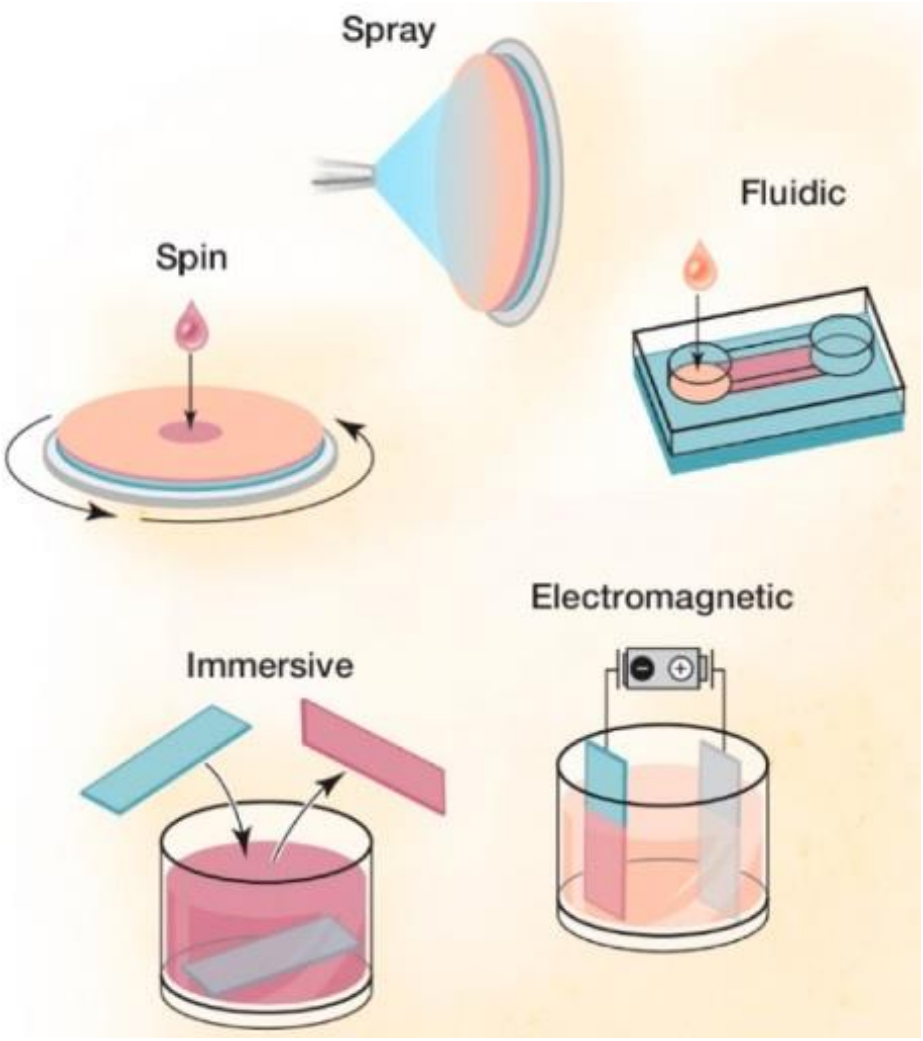

Figure 3.1: Layer-by-layer assembly techniques. Reprinted with permission from [2]. Copyright 2016 American Chemical Society.

Y. Zhang et al., used a LBL approach to deposit a bilayer of graphene oxide (GO) and ethylenediamine (EDA) onto a Torlon polyamideimide hollow fiber support. The bilayers were formed by dip-coating the hollow fiber membrane first in the solution of GO and then EDA. Hyperbranched poly (ethylene imine) was used as the crosslinking agent between GO layer and the substrate. GO aligned themselves orderly in vertical direction due to the exerted surface tension by the coating solution at the hollow fibers and solution interface. Pb (II) rejection % of 95.88+/- 0.93 and 94.57+/-0.57 was obtained for 5 and 10 bilayers respectively [4].

3.1.2. Principle

The formation of LBL systems is driven by factors such oppositely charged electrostatic interactions, hydrogen bonding, hydrophobic interactions, and van der Waals forces. Such assembly can help to tailor properties such as morphology and thickness. The focus of this chapter is an immersive LBL assembly. A typical LBL assembly process consists of formation of multilayer thin films under electrostatic forces by repeatedly immersing a base substrate in two oppositely charged polyelectrolyte solutions. In this technique, a free-standing film is manually immersed in layering solution followed by washing with an appropriate solvent to remove excess and loosened material from the film. Then the original film is further immersed in the next layering solution followed by washing again with appropriate solvent. In this manner, multilayer coatings are performed on a film and the procedure is repeated to get the desired number of multilayers [2, 5, 6].

3.1.3. Goal of our project

In this project, an immersive LBL assembly technique was used to incorporate PA onto a free-standing membrane film. A commercially brought cellulose acetate based membrane film was used as the membrane matrix. A bilayer constituted of an additive solution (CNC, CNF-Amine, and chitosan) and PA solution, was applied alternatively by dipping process. Two and five number of bilayer membrane films were prepared and characterized. Subsequently, the performance of membranes were tested by passing Pb (II) solution through it.

3.2. Materials and Methods

3.2.1. Materials

PA solution 50% (w/w) in H_2O, 1-Methyl-2-pyrrolidinone (NMP), polyvinylpyrrolidone (PVP), chitosan (CHT, 75-85% deacetylated, Mn 50,000 – 190,000 Da), sodium hydroxide (NaOH) and acetone was purchased from Sigma Aldrich. CNC was provided by the University of Maine. CNF-Amine was synthesized according to procedure mentioned by R. Hazra, et al. [7]. Cellulose acetate-based membrane filter (0.8 µm, 47 mm) were purchased from Tisch Scientific.

3.2.2. Preparation of dipped layer by layer using cellulose nanocrystal and phytic acid

An aqueous solution of 1 M NaOH was prepared by dissolving 2 g NaOH in 50 ml water. A solution of CNC was prepared by adding 0.05 g of CNC in 50 ml water. A PA solution was prepared by adding 1 ml of PA in 50 ml water.

A commercially bought cellulose acetate-based membrane was first deacetylated by dipping it in 1 M NaOH solution for 10 min. The first layer over the membrane was prepared by dipping the membrane in CNC solution for 1 min. It was followed by dipping it in water to get rid of loosely held CNC. The second layer over the membrane was prepared by dipping the membrane in PA solution. It was followed by dipping it in water to get rid of loosely held PA. This process was repeated to obtain desired number of bilayers.

3.2.3. Synthesis of CNF-Amine

CNF-Amine was prepared as described in the previous chapter 2, section 2.2.3.

3.2.4. Preparation of dipped layer by layer using CNF-Amine and phytic acid

An aqueous solution of 1 M NaOH was prepared by dissolving 2 g NaOH in 50 ml water. A solution of CNF-Amine was prepared by adding 0.5 g of CNF-Amine in 50 ml water. A PA solution was prepared by adding 1 ml of PA in 50 ml water.

A commercially bought cellulose acetate-based membrane was first deacetylated by dipping it in 1 M NaOH solution for 10 minutes. First layer over the membrane was prepared by dipping the membrane in CNF-Amine solution for 1 minute. It was followed by dipping it in water to get rid of loosely held CNF-Amine. The second layer over the membrane was prepared by dipping the membrane in PA solution. It was followed by dipping it in water to get rid of loosely held PA. This process was repeated to obtain desired number of bilayers.

3.2.5. Preparation of dipped layer by layer using chitosan and phytic acid

An aqueous solution of 1 M NaOH was prepared by dissolving 2 g NaOH in 50 ml water. A solution of chitosan was prepared by adding 0.5 g of chitosan in 50 ml water. To this mixture, an acidic solution of 1 ml water and 0.5 ml acetic acid was added for dissolving

chitosan in water. The pH of this solution was adjusted to 3.0 with HCl. A PA solution was prepared by adding 1 ml of PA in 50 ml water.

A commercially bought cellulose acetate-based membrane was first deacetylated by dipping it in 1 M NaOH solution for 10 minutes. First layer over the membrane was prepared by dipping the membrane in chitosan solution for 1 minute. It was followed by dipping it in water to get rid of loosely held chitosan. The second layer over the membrane was prepared by dipping the membrane in PA solution. It was followed by dipping it in water to get rid of loosely held PA. This process was repeated to obtain desired number of bilayers.

3.3. Characterization Methods

3.3.1. Mechanical properties

The mechanical tests of the composite membranes were conducted according to ASTM D638, with Instron 5542 material testing instrument at temperature of 25°C. In this technique, a specimen is first cut into a specific shape and dimension, and fastened between two grips. It is then subjected to a pulling force until the specimen fractures, and its strength and elongation is determined. The membrane films were cut into Type V dimensions dog bone shape of width 3.18 mm, length 9.53 mm, and the draw speed was set at 0.5 mm/ min. The film was attached between two clamps of the machine. An average of three readings were recorded for tensile strength, tensile strain at break, and young's modulus to determine the mechanical property of the composite membranes.

3.3.2. Porosity and microstructure

Scanning electron microscope was used to capture microscopic images of the membrane films and analyze them on a microscopic scale. In this technique, high energy electron beam is passed through set of lenses on to the sample. The secondary and backscattered electrons generated from the sample is detected by the detector and a microscopic image is produced. Sample material was attached to cylindrical aluminum mounts with carbon adhesive tabs (Ted Pella, Redding, California, USA). Mounted specimens were sputter coated with a conductive layer of gold (Cressington 108auto, Ted Pella, Redding,

California, USA). Images were obtained with a JEOL JSM-6490LV scanning electron microscope (JEOL USA, Inc., Peabody MA, USA).

The pore size of the films was calculated using the software Image J. An SEM image of a particular film was taken as shown in Figure 3.2 a. Circular shapes were drawn over the pores manually to calculate its area. Once all the pores of a particular image were taken into consideration, pore diameters were calculated from its obtained area and a histogram of pores diameter were plotted to calculate its mean diameter (Figure 3.2 b).

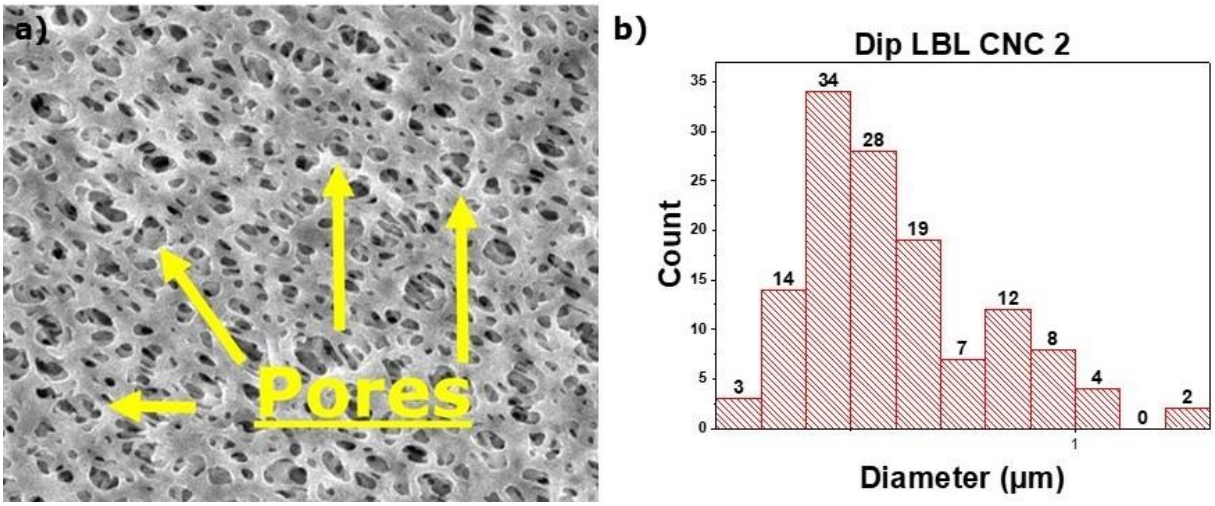

Figure 3.2: SEM image of (a) the membrane film, and (b) histogram of pore size diameter

3.3.3. Surface phosphorus mapping

Energy dispersive X-ray spectroscopy (EDX) technique was used to determine the chemical composition of a material in a particular spot size of few microns in the sample, and to map element composition across a region. Energy-dispersive X-ray information was collected at an accelerating voltage of 15kV using a Thermo Scientific Ultra dry Premium silicon drift detector with NORVAR light element window and Noran System Six imaging system (ThermoFisher Scientific, Madison WI, USA).

3.3.4. Surface elemental composition

X-ray photoelectron spectroscopy (XPS) was carried out to determine the surface elemental composition of the adsorptive membrane. This instrument operates by irradiating

the sample with an X-ray beam, then measuring the kinetic energy and number of electrons rejected. XPS was performed using Thermo Scientific K-Alpha with aluminum anode and the spectra was analyzed on Thermo advantage. The sample was first cleaned by soft argon ion cluster etch for 30 seconds at 4,000 eV. The spot size of the X-ray was 400 micron. The survey scans were run at 200 eV Pass Energy (10 scans each and averaged), 10 ms dwell time with 1.0 eV step size. The Hi resolution scans for P2p were run at 50 eV Pass Energy (10 scans each and averaged), 50 ms dwell time and 0.1 eV step size.

3.3.5. Filtration capacity analysis

Membrane films were cut into circular shape and fitted inside a polypropylene filter assembly of 25 mm diameter. A lead containing solution was prepared of concentration 1 mg Pb/ L of water. 100 ml lead solution was passed through the filter assembly at the flow rate of 0.05 ml min^{-1} cm^{-2} and collected at the end for the evaluation of percentage removal of Pb (II) with Perkin Elmer atomic absorption spectroscopy – PinAAcle 900H. Experiments were conducted in triplicates and averaged out to obtain a mean.

Atomic absorption spectroscopy technique is used to measure trace elements present in a sample. In this technique, the element of interest absorbs light of specific wavelength from the cathode lamp, having a cathode made up of same element as the one being studied. The excited trace metal in the sample, while returning to its ground state, emits light with their characteristic wavelength and intensity, which helps to detect the metal and quantify its concentration.

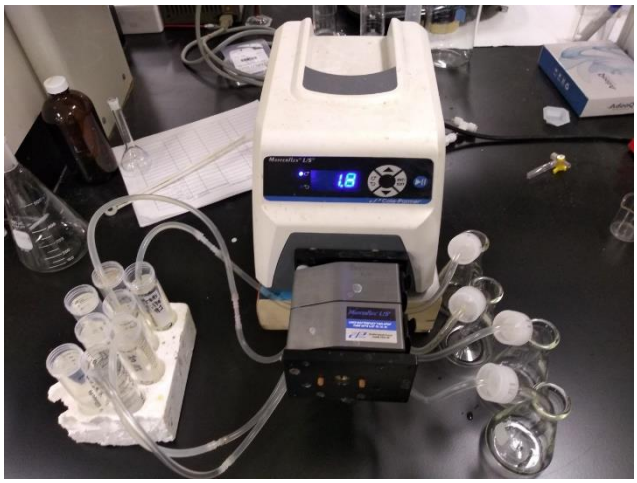

Figure 3.3: Pb (II) ions containing water solution passing through filtration device

3.4. Results and Discussions

3.4.1. Mechanical properties

As can be seen in Figure 3.4, the tensile strength of the membrane is found to decreasing on increasing the number of layers. This might be due to the hydrolysis of the ether bond in cellulose acetate units by aqueous solution of PA occurring during the LBL process, resulting in weakening of tensile strength [8]. On comparing the tensile strength of the three differently treated films, the tensile strength of the films layered with chitosan/ PA is found to be dropped significantly as compared with CNC/ PA and CNF-Amine/ PA. This change in tensile property also resulted in the chitosan/ PA membrane film characteristic to change from soft to brittle.

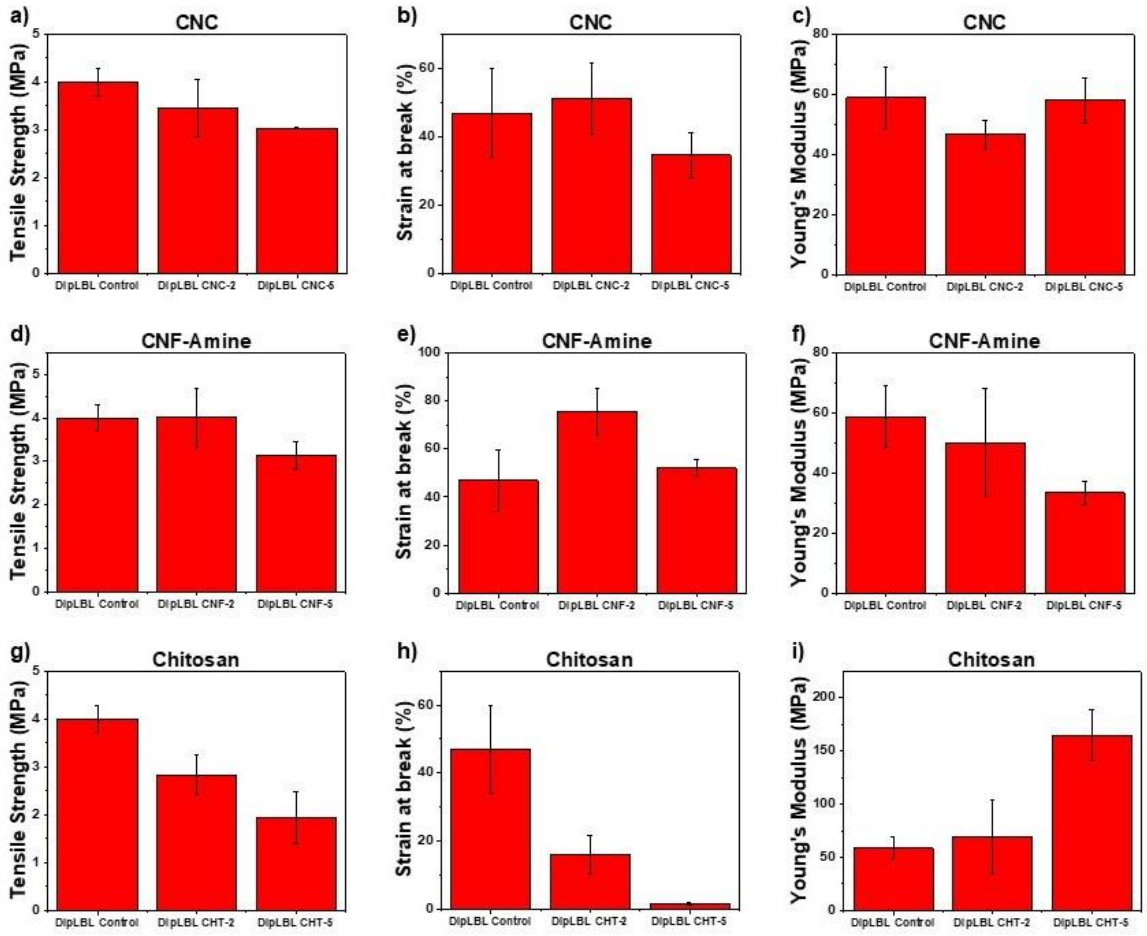

Figure 3.4: Mechanical properties of the membrane films layered with (a - c) CNC/ PA, (d - f) CNF-Amine/ PA, and (g - i) chitosan/ PA

3.4.2. Porosity and microstructure

Figure 3.5 shows that the average pore diameter of the membranes increased as the number of layers applied on the membrane increased from 2 layers to 5 layers. This phenomenon was observed for the films layered with CNC/ PA, CNF-Amine/ PA and also chitosan/ PA. PA can be seen to be destroying the pores of the cellulose acetate based membrane resulting in increased pore size. Such phenomenon has also been observed in PVDF membranes [9].

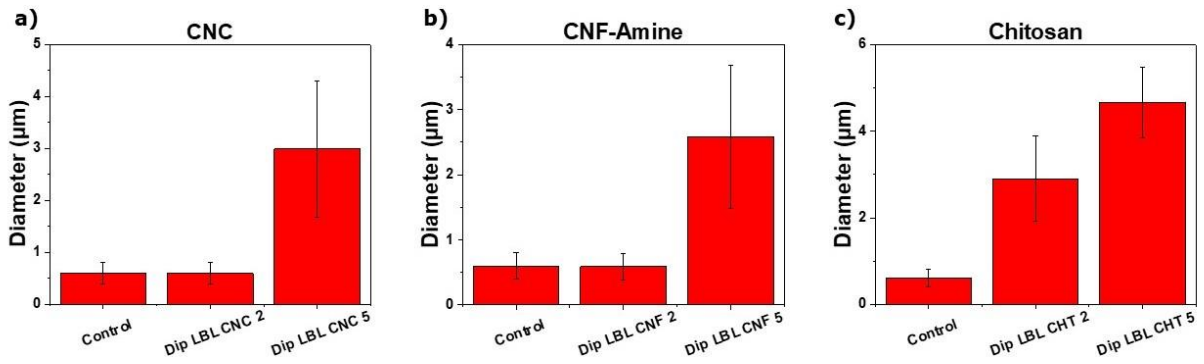

Figure 3.5: Average pore size of the membrane films layered with (a) CNC/ PA, (b) CNF-Amine/ PA, and (c) chitosan/ PA

3.4.3. Surface phosphorus mapping

Energy dispersive X-ray spectroscopy was performed on the membrane film layered with chitosan/ PA to check for the presence of phosphorus. As can be seen in Figure 3.6, the membrane film layered 2x with chitosan/ PA (Figure 3.6 b) and the membrane film layered 5x with chitosan/ PA (Figure 3.6 c) showed significant presence of phosphorus.

The maps obtained from energy dispersive x-ray spectroscopy showed the presence of phosphorus on the surface of the films. However, a minute traces of the yellow spots are from the gold particles that was used to make the surface of the film conductive as can be seen in the control film in Figure 3.6 a. The K_α and the K_β value of phosphorus is 2.010 keV and 2.139 keV that is close to M_α value of gold which is 2.123 keV.

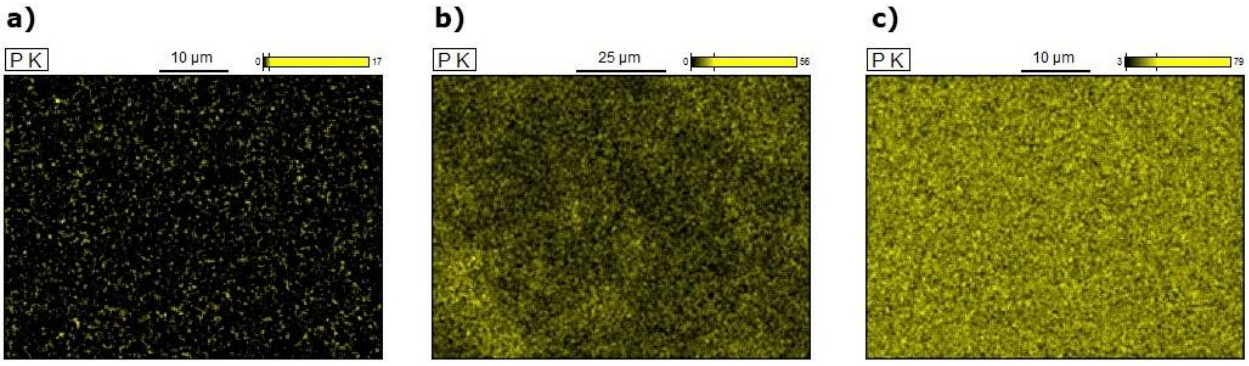

Figure 3.6: Elemental maps of phosphorus on (a) control film, (b) DipLBL CHT-2, and (c) DipLBL CHT-5

3.4.4. Surface elemental composition

The presence of nitrogen, oxygen, carbon, and phosphorus was confirmed by XPS. The phosphorus content in 2 layers film and 5 layers film containing CNC was 0.51 atomic % and 0 atomic % respectively. The phosphorus content in 2 layers film and 5 layers film containing CNF-Amine was 1.125 atomic % and 1.32 atomic % respectively. The phosphorus content in 2 layers film and 5 layers film containing chitosan was 5.91 atomic % and 5.32 atomic % respectively. The low presence of phosphorus on the membrane film layered with CNC/ PA and CNF-Amine/ PA may be due to the weak interfacial adhesion of CNC and CNF-Amine with the cellulose acetate membrane matrix that does not allow PA to deposit on the surface of the film. The successful presence of phosphorus on the film layered with chitosan/ PA is attributed to the ionic complexation of positively charged chitosan and negatively charged PA [10, 11]. Therefore, the intensity of the phosphorus peaks in chitosan/ PA (Figure 3.7 c) is the highest followed by CNF-Amine/ PA (Figure 3.7 b), and CNC/ PA (Figure 3.7 a). The peak signals are also observed to plateau or drop as the number of layers increases. That explains the limitations of the membrane film towards loading of the PA on the surface of the film.

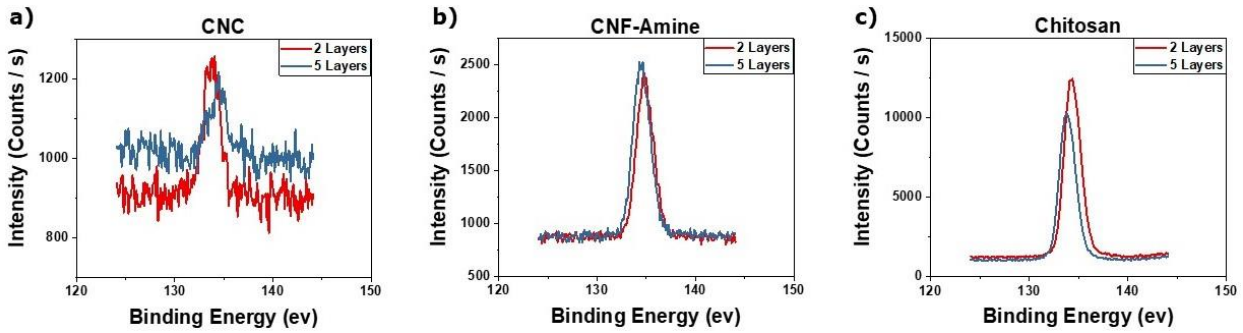

Figure 3.7: Phosphorus content on the films layered with (a) CNC/ PA, (b) CNF-Amine/ PA, and (c) Chitosan/ PA

3.4.5. Filtration capacity evaluation

The control films removes certain amount of Pb (II) ions because of the electrostatic force between the Pb (II) ions and the ester group oxygen atoms in the cellulose acetate [12]. The films coated with chitosan/ PA removed up to 90% of Pb (II) ions from the water solution.

The increase in the adsorption of Pb (II) for the films coated with chitosan/ PA (Figure 3.8 c) is due to the introduction of nitrogen and oxygen containing functional group from chitosan, and PA. The Pb (II) removal capacity also correlates with XPS data of phosphorus presented in the section 3.4.4. This explains the successful immobilization of PA onto the chitosan/ PA layered membrane film and effective removal of Pb (II) ions from water.

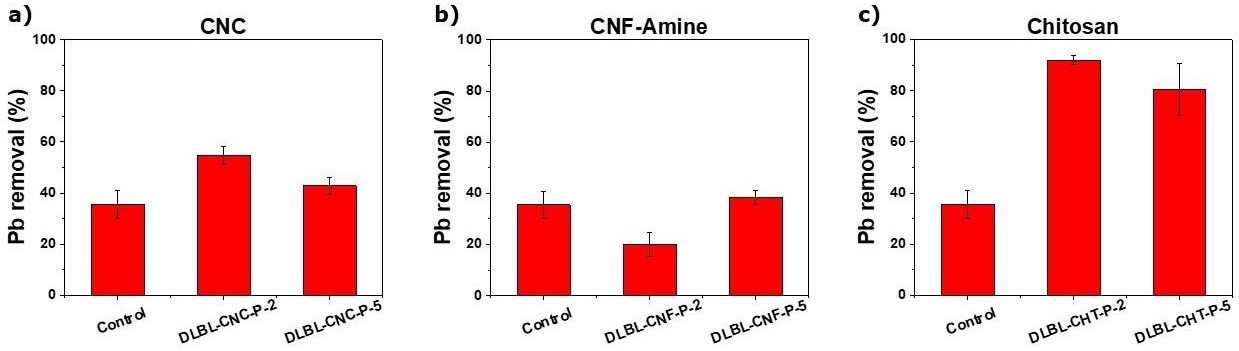

Figure 3.8: % Pb (II) removal by membrane films layered with (a) CNC/ PA, (b) CNF-Amine/ PA, and (c) chitosan/ PA

3.5. Conclusion

In conclusion, the films layered with chitosan/ PA performed twice as better in removing Pb (II) ions from water solution in relation to the films layered with CNC/ PA and CNF-Amine/ PA. Chitosan/ PA layered membrane films showed up to 90% efficiency in removing Pb (II) ions from water solution. This observation was mainly attributed to the adsorption of Pb (II) ions by PA that is adhered to the cellulose acetate-based membrane film with the help of chitosan. The same results were not found in the case of CNC/ PA and CNF-Amine/ PA because CNC and CNF-Amine does not adhere well to the cellulose acetate-based membrane surface due to weak interfacial interaction and PA directly does not form a strong bond with the membrane film surface. However, despite this successful Pb (II) ion removal result by the membrane layered with chitosan/ PA, the film itself diminishes down in its mechanical strength as the layering treatment on the film is increased, making it mechanically unstable. This could be due to the breakage of the ether bonds on the support membrane

that results in increased porosity, and the changing characteristic on the film from soft to brittle upon drying.

3.6. Overall Conclusion

We found that the cellulose acetate based membrane films blended with CNC and prepared using immersion precipitation method, performed three fold better at removing Pb (II) ions from water solution than those containing CNF-amine and chitosan. The removal efficiency of up to 60% was achieved with the membrane films blended with CNC. The reason for the removal of Pb (II) by the CNC containing membrane could be due to the chelation of Pb (II) ions by the phosphate groups of PA combined with the electrostatic attraction of Pb (II) ions with the hydroxyl group in CNC. The removal of Pb (II) ions was not so evident in case of CNF-amine, and chitosan. That could be because of the unavailability of the phosphate groups of the PA, as those phosphate groups would be electrostatically complexed with amines of CNF-amine and chitosan.

While in the case of commercially available cellulose acetate based membrane films, we found that the membrane films layered with chitosan/ PA performed better at removing Pb (II) from water solution that the membrane films layered with CNC/ PA and CNF-amine/ PA. The removal efficiency of up to 90% was achieved with the membrane films coated with chitosan/ PA. This removal mechanism was attributed to the chelating effect of PA with Pb (II).

3.7. Challenges and Future Outlook

In NIPS method, Since the amount of PA loaded into films is less than 10% of the feed amount of PA, we assume that most of PA is lost during the processing and fabrication of the films. That explains that our synthesis technique has a low atom economy, which results in a large amount of waste, and calls for improvement of processing conditions in future efforts. We could also focus on modifying the chemistry of PA to covalently link the acid to membrane scaffolds to increase PA content in the film. Improving the retention quantity of PA in the membrane could also potentially improve the membranes efficiency in removing Pb (II) ions

from water. NIPS method is fundamentally associated with waste generation and recycling – a challenge that needs to be tackled as far industrial scaling up is concerned [13].

In the dipped LBL technique, the physical characteristic of the film was found to be deteriorating as the amount of layers of chitosan/ PA was increasing. So, work towards functionalizing the membrane film while maintaining its integrity can be looked into. In addition, we also faced issue of cross-contamination while transferring membrane film from one solution to another. Therefore, there is an opportunity to improve the product and the synthesis processes from the aspect of green chemistry principles.

3.8. References

[1] X. Wang, Y. Zhao, E. Tian, J. Li, and Y. Ren, "Graphene Oxide-Based Polymeric Membranes for Water Treatment," *Advanced Materials Interfaces,* vol. 5, no. 15, p. 1701427, 2018/08/01 2018, doi: 10.1002/admi.201701427.

[2] J. J. Richardson, J. Cui, M. Björnmalm, J. A. Braunger, H. Ejima, and F. Caruso, "Innovation in Layer-by-Layer Assembly," *Chemical Reviews,* vol. 116, no. 23, pp. 14828-14867, 2016/12/14 2016, doi: 10.1021/acs.chemrev.6b00627.

[3] S. Gao, Y. Zhu, J. Wang, F. Zhang, J. Li, and J. Jin, "Layer by Layer Construction of Cu2+/Alginate Multilayer Modified Ultrafiltration Membrane with Bioinspired Superwetting Property for High Efficient Crud… OiŒ i□ Water Emulsion Separation," *Advanced Functional Materials,* vol. 28, p. 1801944, 2018.

[4] Y. Zhang, S. Zhang, J. Gao, and T. S. Chung, "Layer-by-layer construction of graphene oxide (GO) framework composite membranes for highly efficient heavy metal removal," *Journal of Membrane Science,* vol. 515, pp. 230-237, 2016/10/01/ 2016, doi: https://doi.org/10.1016/j.memsci.2016.05.035.

[5] P. T. Hammond, "Form and Function in Multilayer Assembly: New Applications at the Nanoscale," *Advanced Materials,* https://doi.org/10.1002/adma.200400760 vol. 16, no. 15, pp. 1271-1293, 2004/08/04 2004, doi: https://doi.org/10.1002/adma.200400760.

[6] M. M. de Villiers, D. P. Otto, S. J. Strydom, and Y. M. Lvov, "Introduction to nanocoatings produced by layer-by-layer (LbL) self-assembly," *Advanced Drug Delivery Reviews,* vol. 63, no. 9, pp. 701-715, 2011/08/14/ 2011, doi: https://doi.org/10.1016/j.addr.2011.05.011.

[7] R. S. Hazra *et al.*, "Cellulose Mediated Transferrin Nanocages for Enumeration of Circulating Tumor Cells for Head and Neck Cancer," *Scientific Reports,* vol. 10, no. 1, p. 10010, 2020/06/19 2020, doi: 10.1038/s41598-020-66625-2.

[8] X. W. Cheng, R. C. Tang, J. P. Guan, and S. Q. Zhou, "An eco-friendly and effective flame retardant coating for cotton fabric based on phytic acid doped silica sol approach," *Progress in Organic Coatings,* vol. 141, p. 105539, 2020/04/01/ 2020, doi: https://doi.org/10.1016/j.porgcoat.2020.105539.

[9] X. Zeng *et al.*, "Fabrication of superhydrophilic PVDF membranes by one-step modification with eco-friendly phytic acid and polyethyleneimine complex for oil-in-water emulsions separation," *Chemosphere,* vol. 264, p. 128395, 2021/02/01/ 2021, doi: https://doi.org/10.1016/j.chemosphere.2020.128395.

[10] T. Zhang *et al.*, "Chitosan/Phytic Acid Polyelectrolyte Complex: A Green and Renewable Intumescent Flame Retardant System for Ethylene–Vinyl Acetate Copolymer," *Industrial & Engineering Chemistry Research,* vol. 53, no. 49, pp. 19199-19207, 2014/12/10 2014, doi: 10.1021/ie503421f.

[11] Z. Zhang, X. Li, Z. Ma, H. Ning, D. Zhang, and Y. Wang, "A facile and green strategy to simultaneously enhance the flame retardant and mechanical properties of poly(vinyl alcohol) by introduction of a bio-based polyelectrolyte complex formed by chitosan and phytic acid," *Dalton Transactions,* 10.1039/D0DT02019B vol. 49, no. 32, pp. 11226-11237, 2020, doi: 10.1039/D0DT02019B.

[12] M. A. O. Iqhrammullah *et al.*, "Characterization and Performance Evaluation of Cellulose Acetate-Polyurethane Film for Lead II Ion Removal. LID - 10.3390/polym12061317 [doi] LID - 1317," (in eng), no. 2073-4360 (Electronic).

[13] J. Richardson, M. Björnmalm, and F. Caruso, "Technology-driven layer-by-layer assembly of nanofilms," *Science,* vol. 348, 2015.